Advances in Computational Mathematics (2026) 52:17
https://doi.org/10.1007/s10444-026-10288-6

A posteriori error estimates for a C^1 virtual element method applied to the thin plate vibration problem.

Franco Dassi[1] · Andrés E. Rubiano[2] · Iván Velásquez[3]

Received: 31 July 2025 / Accepted: 29 January 2026
© The Author(s) 2026

Abstract
We propose and analyse residual-based a posteriori error estimates for the virtual element discretisation applied to the thin plate vibration problem in both two and three dimensions. Our approach involves a conforming C^1 discrete formulation suitable for meshes composed of polygons and polyhedra. The reliability and efficiency of the error estimator are established through a dimension-independent proof. Finally, several numerical experiments are reported to demonstrate the optimal performance of the method in 2D and 3D.

Keywords A posteriori error analysis in 2D and 3D · Virtual element method · Kirchhoff plates · Vibration spectral problem

Mathematics Subject Classification (2010) 65F15 · 65N25 · 65N50 · 74K20

1 Introduction

In this paper, we propose and develop a posteriori error estimates for the vibration problem of a thin plate modeled by the Kirchhoff-Love equations. In particular, given

Communicated by: Ilaria Perugia

✉ Iván Velásquez
ivan.velasquez@unimilitar.edu.co

Franco Dassi
franco.dassi@unimib.it

Andrés E. Rubiano
andres.rubianomartinez@monash.edu

1 Dipartimento di Matematica e Applicazioni, Università degli studi di Milano - Bicocca, Via Roberto Cozzi 55, 20125 Milano, Italy

2 School of Mathematics, Monash University, 9 Rainforest Walk, VIC 3800 Melbourne, Australia

3 Departamento de Matemáticas, Universidad Militar Nueva Granada, Bogotá, Colombia

Published online: 23 February 2026

a bounded simply-connected Lipschitz domain $\Omega \subseteq \mathbb{R}^d$ $(d = 2, 3)$ with boundary $\Gamma := \partial\Omega$. The deflection $u : \mathbb{R}^d \to \mathbb{R}$ and the vibration frequency $\omega > 0$ satisfy the following eigenvaule problem, with $\lambda = \omega^2$.

$$\begin{cases} \Delta^2 u = \lambda u, & \text{in } \Omega, \\ \mathcal{B}^j u = 0, & \text{on } \Gamma, \end{cases} \tag{1}$$

where $\Delta^2 u := \Delta(\Delta u)$ denotes the fourth-order biharmonic operator. We also introduce the Hessian matrix, which consists of all second-order partial derivatives of u, denoted by $\nabla^2 u$.

On the other hand, the linear differential operator $\mathcal{B}^j$ $(j = 1, 2)$ involves partial derivatives of the function u (e.g. [1, Section 2.3]). Specifically, let $\boldsymbol{n}$ be the outward unit normal vector to Γ, and $\partial_{\boldsymbol{n}}$ the normal derivative. We consider two types of homogeneous boundary conditions:

- **Simply supported plate (SSP):**

$$\mathcal{B}^j u := \Delta^{j-1} u = 0 \quad \text{on } \Gamma \quad \text{for } j = 1, 2. \tag{2}$$

- **Clamped plate (CP):**

$$\mathcal{B}^j u := \partial_{\boldsymbol{n}}^{j-1} u = 0 \quad \text{on } \Gamma \quad \text{for } j = 1, 2. \tag{3}$$

Numerical methods for eigenvalue problems are a subject of active research, among both practical applications [2], and theoretical analysis [3, 4]. In particular, conforming finite element methods have been proposed to get the solution of this problem. However, due to the C^1 continuity requirement, it is well known that a high polynomial degree is required to achieve conformity in the discrete space [5], which leads to an important computational effort. To avoid this issue, we mention some alternatives applied to the thin plate vibration problem, such as non-conforming methods [5–7], discontinuous schemes [8, 9], and mixed formulations [10–12].

The Virtual Element Method (VEM), first introduced in [13, 14], has the flexibility to be applied to more general polygonal/polytopal meshes, and by construction, one can define high regular discrete spaces [15]. Moreover, C^1-conforming VEM spaces necessitate only 3 degrees of freedom (DoFs) per vertex when Ω is a bidimensional domain, and 4 DoFs for the three-dimensional case, providing an efficient way to retain the accuracy of the method at low computational cost. We provide a brief, non-exhaustive overview of VEM discretisations for equations involving the biharmonic operator [16–20], and different eigenvalue problems [21–30].

Adaptive schemes driven by a posteriori error estimators allow optimal convergence recovery in cases such as singular solutions and complex geometries (e.g. non-convex domains and sharp corners). We refer to [31–34] for previous work on adaptive FEM for the biharmonic problem. The main advantage of VEMs is its natural handling of hanging nodes during adaptive mesh refinement algorithms, [35–39] provide some examples on adaptive VEMs.

Our goal here is to derive a reliable and efficient a posteriori global error estimator η for (1), i.e. the following property holds for η:

$$C_1(\text{error} + \text{oscillation terms}) \leq \eta \leq C_2(\text{error} + \text{oscillation terms} + \text{higher-order terms}).$$

Typically, oscillation terms appear in virtual element methods due to the projection and stabilisation required to achieve the computability of virtual functions. On the other hand, high-order terms are negligible when $h \to 0$.

We point out that the a priori error analysis of a virtual element method for the vibration eigenvalue problem in two and three dimensions was analyzed in [30] and [22], respectively. However, in this work, some additional a priori estimates are presented that will be fundamental for the a posteriori analysis of the model problem (1). In addition, to the best of our knowledge, this is the first study of an a posteriori error estimation by means of a C^1-virtual element for the vibration eigenvalues problem in two and three dimensions.

Main contributions

- Design of a reliable and efficient residual-based a posteriori error estimator for the thin plate vibration problem in 2D and 3D.
- Open-source implementation of the method, available in the `VEM++` library [40] for polytopal meshes.
- Several numerical experiments that confirm the theoretical results, including: uniform vs adaptive mesh refinement test to show the optimal performance of the error and a posteriori error estimator in both 2D and 3D, analysis of the influence of the stabilisation terms. Additionally, we consider the vibration problem on an aircraft wing as a relevant application.

Plan of the paper The contents of this paper are organised as follows. The remainder of this section contains preliminary notational conventions. Section 2 presents the continuous spectral formulation for the vibration problem and provides the spectral characterisation for the eigenvalues. The virtual element space, along with its spectral properties and error estimates, are provided in Sections 3 and 4, respectively. Section 5 is devoted to deriving a reliable and efficient residual-type estimator. Finally, our theoretical results are illustrated via numerical examples in Section 6.

Recurrent notation Throughout this paper, we shall use standard notations for Sobolev spaces, norms, and semi-norms as in [41]. The notation $a \lesssim b$ means that there exists a positive constant C independent of the mesh size h and dimension d (which can take different values in each case) such that $a \leq Cb$.

2 The continuous spectral weak formulations

In this section, we introduce two continuous variational formulations associated with the vibration problems of a simply supported and clamped plate (1).

- **SSP:** Find $(\lambda, u) \in \mathbb{R} \times \left(H^2(\Omega) \cap H_0^1(\Omega)\right)$, with $u \neq 0$ such that

$$\int_\Omega \nabla^2 u : \nabla^2 v \, d\Omega = \lambda \int_\Omega uv \, d\Omega \qquad \forall v \in H^2(\Omega) \cap H_0^1(\Omega). \tag{4}$$

- **CP:** Find $(\lambda, u) \in \mathbb{R} \times H_0^2(\Omega)$, with $u \neq 0$ such that

$$\int_\Omega \nabla^2 u : \nabla^2 v \, d\Omega = \lambda \int_\Omega uv \, d\Omega \qquad \forall v \in H_0^2(\Omega). \tag{5}$$

For notational convenience, we introduce the following bilinear forms:

$$a : H^2(\Omega) \times H^2(\Omega) \to \mathbb{R}, \qquad a(u, v) := \int_\Omega \nabla^2 u : \nabla^2 v \, d\Omega \,, \tag{6}$$

$$b : L^2(\Omega) \times L^2(\Omega) \to \mathbb{R}, \qquad b(u, v) := \int_\Omega u \, v \, d\Omega \,. \tag{7}$$

Since the bilinear form $a(\cdot, \cdot)$ is elliptic in both $H^2(\Omega) \cap H_0^1(\Omega)$ and $H_0^2(\Omega)$ spaces, then the analysis for the problems (4) and (5) can be developed using the same arguments. Therefore, from now on, we write V to refer to both spaces. In what follows, we are interested in approximating the eigenpair of the following spectral problem.

Problem 1 Find $(\lambda, u) \in \mathbb{R} \times V$, with $u \neq 0$ such that

$$a(u, v) = \lambda b(u, v), \qquad \forall v \in V.$$

2.1 The source problems

To deal with the a priori and a posteriori error analysis for the spectral Problem 1, we define the following solution operators

$$T : V \to V, \quad f \longmapsto w,$$
$$T^0 : L^2(\Omega) \to V \subseteq L^2(\Omega), \quad f^0 \longmapsto w^0,$$

where $w := Tf$ and $w^0 := T^0 f$ are the two unique solutions associated with their respective source problems

$$a(w, v) = b(f, v), \qquad \forall v \in V, \tag{8}$$

$$a(w^0, v) = b(f^0, v), \qquad \forall v \in V. \tag{9}$$

It is well known that forms $a(\cdot, \cdot)$ and $b(\cdot, \cdot)$ satisfy the Lax-Milgram theorem. Therefore, the linear operators T and T^0 are well defined and bounded. Moreover, the following results are standard in the literature of spectral theory of operators in Banach spaces (e.g. [6]).

Proposition 1 *$(\lambda, u) \in \mathbb{R} \times V$ is a eigenpair of Problem 1 with $u \neq 0$ and $\lambda \neq 0$ if and only if $(\mu, u) \in \mathbb{R} \times V$ is a eigenpair of T, where $u \neq 0$ and $\mu := 1/\lambda$.*

Proposition 2 *The operators T and T^0 are self-adjoint with respect to the inner products $a(\cdot,\cdot)$ in V and $b(\cdot,\cdot)$ in $L^2(\Omega)$, respectively.*

Proof Given v, $f \in V$, and f^0, $g^0 \in L^2(\Omega)$, we readily see that

$$a(Tf, v) = b(f, v) = b(v, f) = a(Tv, f) = a(f, Tv),$$
$$b(T^0 f^0, g^0) = b(g^0, T^0 f^0) = a(T^0 g^0, T^0 f^0) = a(T^0 f^0, T^0 g^0) = b(f^0, T^0 g^0).$$

□

We conclude this section by recalling the spectral characterisation of the vibration problem of a thin plate modeled by the Kirchhoff-Love equations (see, for instance, [6, 30]).

Theorem 3 *The spectrum of the operators T and T^0 denoted by* $\mathrm{sp}(T)$ *and* $\mathrm{sp}(T^0)$*, respectively, satisfy:*

$$\mathrm{sp}(T) = \{0\} \cup \{\mu_k\}_{k\in\mathbb{N}} = \mathrm{sp}(T^0), \quad \{\mu_k\}_{k\in\mathbb{N}} \subset (0, \infty) \quad \textit{and} \quad \lim_{k\to\infty} \mu_k = 0.$$

Moreover, each eigenvalue μ_k has finite multiplicity.

3 The virtual spectral approximation

Let $\{\Omega_h\}_h$ be a sequence of decompositions of Ω into polygons K. Let h_K denote the diameter of the element K and $h := \max_{K\in\Omega_h} h_K$. Similar to [13], we assume that there exists a positive constant C_Ω such that

- **(A1)** The ratio between the shortest edge and the diameter h_K of K is larger than C_Ω.
- **(A2)** Every polygon $K \in \Omega_h$ is star-shaped with respect to a ball with radius $C_\Omega h_K$.

In what follows, we denote by N_K the number of vertices of K, l denotes a generic edge of Ω_h and for all $l \in \partial K$, we define a unit normal vector $\boldsymbol{n}_K^l$ that points outside of K. Moreover, for any polygon $K \in \Omega_h$ we denote by $\mathcal{E}_K$ the set of edges of K and $\mathcal{E} := \bigcup_{K\in\Omega_h} \mathcal{E}_K$. We also introduce the sets $\mathcal{E}_\Gamma := \{l \in \mathcal{E} : l \subset \Gamma\}$, and $\mathcal{E}_\Omega := \mathcal{E}\backslash\mathcal{E}_\Gamma$. In addition, given $\mathcal{O} \subseteq \mathbb{R}^d$, we denote the polynomial space in d-variables of degree lower or equal to k as $\mathbb{P}_k(\mathcal{O})$. Finally, for all $K \in \Omega_h$, we introduce the broken H^2-seminorm given by

$$|v|_{2,h}^2 := \sum_{K\in\Omega_h} |v|_{2,K}^2.$$

Next, for all polygon $K \in \Omega_h$, we consider the local virtual space

$$\widetilde{V}_K := \Big\{ v_h \in H^2(K) : \Delta^2 v_h \in \mathbb{P}_2(K), \\ v_h|_{\partial K} \in C^0(\partial K),\ v_h|_l \in \mathbb{P}_3(l), \forall l \in \partial K, \\ \nabla v_h|_{\partial K} \in C^0(\partial K)^2,\ \partial_{\boldsymbol{n}_K^l} v_h|_l \in \mathbb{P}_1(l), \forall l \in \partial K \Big\}.$$

From here, the enhanced local virtual space is given by

$$V_h^K := \left\{ v_h \in \widetilde{V}_K : \int_K (\Pi_K^\Delta v_h) p_2 \, dK = \int_K v_h p_2 \, dK,\ \forall p_2 \in \mathbb{P}_2(K) \right\},$$

where the polynomial projection operator $\Pi_K^\Delta : \widetilde{V}_K \to \mathbb{P}_2(K) \subseteq \widetilde{V}_K$ is defined as follows:

$$\begin{cases} \displaystyle\int_K \nabla^2(\Pi_K^\Delta v_h - v_h) \cdot \nabla^2 p_2 \, \mathrm{d}K = 0, \quad \forall p_2 \in \mathbb{P}_2(K), \\ \displaystyle\int_{\partial K} (\Pi_K^\Delta v_h - v_h) p_1 \, \mathrm{d}l = 0, \quad \forall p_1 \in \mathbb{P}_1(\partial K). \end{cases}$$

We are ready to present the global virtual space: for every decomposition Ω_h of Ω into simple polygons K, we define

$$V_h := \left\{ v_h \in V :\ v_h|_K \in V_h^K \right\}.$$

It is well known (see [18]) that any virtual function $v_h \in V_h^K$ and $\Pi_K^\Delta v_h$ are uniquely determined by the following degrees of freedom:

$$\mathbf{D_1} : \text{Evaluation of } v_h \text{ at the vertexes of } K,$$
$$\mathbf{D_2} : \text{Evaluation of } \nabla v_h \text{ at the vertexes of } K.$$

Notice that this definition implies that only three DoFs per vertex are required for this space. In order to write the discrete spectral problem, we define

$$a_h(u_h, v_h) := \sum_{K \in \Omega_h} a_{h,K}(u_h, v_h), \qquad b_h(u_h, v_h) := \sum_{K \in \Omega_h} b_{h,K}(u_h, v_h), \qquad \forall u_h, v_h \in V_h,$$

where $a_{h,K}(\cdot,\cdot)$ and $b_{h,K}(\cdot,\cdot)$ are the local discrete bilinear forms on $V_h^K \times V_h^K$ given by

$$\begin{aligned} a_{h,K}(u_h, v_h) &:= a_K\left(\Pi_K^\Delta u_h, \Pi_K^\Delta v_h\right) + s_K^\Delta\left(u_h - \Pi_K^\Delta u_h, v_h - \Pi_K^\Delta v_h\right), \quad \forall u_h, v_h \in V_h^K, \\ b_{h,K}(u_h, v_h) &:= b_K\left(\Pi_K^0 u_h, \Pi_K^0 v_h\right) + s_K^0\left(u_h - \Pi_K^0 u_h, v_h - \Pi_K^0 v_h\right), \quad \forall u_h, v_h \in V_h^K, \end{aligned} \tag{10}$$

with $\Pi_K^0 : L^2(K) \to \mathbb{P}_2(K)$ is the standard L^2-projection and s_K^Δ and s_K^0 are any symmetric positive bilinear forms satisfying

$$\alpha_* a_K(v_h, v_h) \le s_K^\Delta(v_h, v_h) \le \alpha^* a_K(v_h, v_h), \quad \forall v_h \in V_h^K \cap \ker(\Pi_K^\Delta),$$
$$\beta_* b_K(v_h, v_h) \le s_K^0(v_h, v_h) \le \beta^* b_K(v_h, v_h), \quad \forall v_h \in V_h^K \cap \ker(\Pi_K^0),$$

with $\alpha_*, \alpha^*, \beta_*$ and β^* positive constants independent of h_K.

Remark 1 The polynomial projections $\Pi_K^\Delta v_h$ and $\Pi_K^0 v_h$ coincide in the lowest order case, for all $v_h \in V_h^K$ (see [30]).

Lemma 4 *Let $h > 0$. For all polygon $K \in \Omega_h$ the following relations hold true:*

$$a_{h,K}(p_2, v_h) = a_K(p_2, v_h), \quad \forall p_2 \in \mathbb{P}_2(K), \quad \forall v_h \in V_h^K,$$
$$b_{h,K}(p_2, v_h) = b_K(p_2, v_h), \quad \forall p_2 \in \mathbb{P}_2(K), \quad \forall v_h \in V_h^K,$$

and

$$\min\{1, \alpha_*\} a_K(v_h, v_h) \le a_{K,h}(v_h, v_h) \le \max\{1, \alpha^*\} a_K(v_h, v_h), \quad \forall v_h \in V_h(K) \cap \ker(\Pi_K^\Delta),$$
$$\min\{1, \beta_*\} b_K(v_h, v_h) \le b_{K,h}(v_h, v_h) \le \max\{1, \beta^*\} b_K(v_h, v_h), \quad \forall v_h \in V_h(K) \cap \ker(\Pi_K^0).$$

Remark 2 Lemma 4 implies that the discrete forms $a_h(\cdot, \cdot)$ and $b_h(\cdot, \cdot)$ satisfy the Lax-Milgram theorem.

3.1 Discrete spectral formulation

The virtual element discretization of problem (1) can be read as follows.

Problem 2 Find $(\lambda_h, u_h) \in \mathbb{R} \times V_h$, with $u_h \neq 0$ such that

$$a_h(u_h, v_h) = \lambda_h b_h(u_h, v_h) \qquad \forall v_h \in V_h.$$

Following Section 2.1, we introduce the discrete solution operator

$$T_h : V_h \to V_h \subseteq V, \quad f_h \longmapsto w_h,$$

where $w_h := T_h f_h$ is the unique solution of the source problem

$$a_h(w_h, v_h) = b_h(f_h, v_h) \qquad \forall v_h \in V_h\,. \tag{11}$$

From Remark 2, the solution operator T_h is well defined and bounded. In addition, following the same arguments as in the continuous case, T_h is a self-adjoint operator with respect to the inner product $a_h(\cdot, \cdot)$. Moreover, the spectral characterisation for operator T_h is summarised in the following result.

Theorem 5 *The spectrum of T_h is given by* $\mathrm{sp}(T_h) = \{\mu_{jh}\}_{j=1}^{\dim V_h} \subset (0, \infty)$, *where each μ_{jh} is repeated according to their multiplicities.*

4 A priori error analysis

This section focuses on presenting a measured error estimation result in the L^2-norm for the eigenfunctions of the vibration problem of a thin plate. This result will be important for the a posteriori error analysis in the following section.

We start by recalling some well-known interpolation theorems commonly used in the literature on virtual element methods.

Proposition 6 *Assume that assumption* **A2** *holds true. Then, for all* $v \in H^{2+s}(K)$ *with* $s \in (1/2, 1]$, *there exists* $v_\pi \in \mathbb{P}_2(K)$ *satisfying*

$$|v - v_\pi|_{\ell,K} \lesssim h_K^{2+s-\ell} |v|_{2+s,K}, \quad \ell = 0, 1, 2.$$

Proposition 7 *Assume that assumption* ***A1–A2*** *hold true. Then, for all* $v \in H^{2+s}(\Omega)$ *with* $s \in (1/2, 1]$ *there exist* $v_I \in V_h$ *such that*

$$\|v - v_I\|_{2,\Omega} \lesssim h^s |v|_{2+s,\Omega}.$$

Remark 3 We will prove the convergence in V-norm of $T_h \to T$. For this end, we will employ the spectral theory for compact operators established in [6]. However, since stabilisation terms $s^0(\cdot, \cdot)$ needs the dofs $\mathbf{D_1}$ and $\mathbf{D_2}$ on the right-hand side of (11) the operator T_h is not well defined for all $f \in V$. To overcome this issue, we consider the orthogonal projection $\mathcal{P}_h : L^2(\Omega) \to V_h$ given by $f \mapsto \mathcal{P}_h f$ as the unique solution of the following system of equations

$$b(\mathcal{P}_h f - f, v_h) = 0, \quad \forall v_h \in V_h.$$

Moreover, for all $f \in L^2(\Omega)$ the following holds

$$||f - \mathcal{P}_h f||_{0,\Omega} = \inf_{v_h \in V_h} ||f - v_h||_{0,\Omega}, \quad \forall v_h \in V_h.$$

Next, we introduce the projector $\widehat{T}_h := T_h \mathcal{P}_h : V \to V_h \subseteq V$. Then, the spectrum of $\widehat{T}_h$ satisfies $\mathrm{sp}(\widehat{T}_h) = \mathrm{sp}(T_h) \cup \{0\}$ and the eigenfunctions of operators $\widehat{T}_h$ and T are the same (e.g. [42]). Now, the following result establishes the convergence of $\widehat{T}_h \to T$ and $\widehat{T}_h \to T^0$ when $h \to 0$.

Lemma 8 *Given* $s \in (1/2, 1]$ *the following bounds hold*

$$||(T - \widehat{T}_h) f||_{2,\Omega} \lesssim h^s ||f||_{2,\Omega}, \quad \forall f \in V, \tag{12a}$$

$$||(T^0 - \widehat{T}_h) f||_{0,\Omega} \lesssim h^s ||f||_{0,\Omega}, \quad \forall f \in L^2(\Omega). \tag{12b}$$

Proof The proof for (12a) was established in [30] (see also [22, Proposition 5]). Now, let us prove (12b). Given $f \in L^2(\Omega)$, consider $T^0 f = w^0 \in V$ and $\widehat{T}_h f = T_h \mathcal{P}_h f = w_h \in V_h$ as the unique solutions of the source problems $a(w^0, v) = b(f, v)\ \forall v \in V$,

(cf. (9)) and $a_h(w_h, v_h) = b_h(\mathcal{P}_h f, v_h)\ \forall v_h \in V_h$ (cf. (11)), respectively. Then, by using the same steps as those applied in [22, Theorem 5.1], we obtain

$$|w^0 - w_h|^2_{2,\Omega} \leq b_h(\mathcal{P}_h f, v_h) - b(f, v) - \sum_{K\in\Omega_h} \Big\{a_{h,K}(w_I^0 - w_\pi^0, v_h) + a_K(w_\pi^0 - w^0, v_h)\Big\}. \tag{13}$$

Note that

$$\begin{aligned}
b_h(\mathcal{P}_h f, v_h) - b(f, v) &= \sum_{K\in\Omega_h} \Big\{b_{h,K}(\mathcal{P}_h f, v_h - (v_h)_\pi) - b_K(f, v_h) + b_{h,K}(\mathcal{P}_h f, (v_h)_\pi)\Big\} \\
&= \sum_{K\in\Omega_h} \Big\{b_{h,K}(\mathcal{P}_h f, v_h - (v_h)_\pi) - b_K(\mathcal{P}_h f, v_h) + b_{h,K}(\mathcal{P}_h f, (v_h)_\pi)\Big\} \\
&= \sum_{K\in\Omega_h} \Big\{b_{h,K}(\mathcal{P}_h f, v_h - (v_h)_\pi) - b_K(\mathcal{P}_h f, v_h - (v_h)_\pi)\Big\} \\
&\lesssim \Big(\sum_{K\in\Omega_h} ||\mathcal{P}_h f||^2_{0,K}\Big)^{1/2} \Big(||v_h - (v_h)_\pi||^2_{0,K}\Big)^{1/2} \\
&\lesssim \Big(\sum_{K\in\Omega_h} ||\mathcal{P}_h f||^2_{0,K}\Big)^{1/2} h^2 ||v_h||_{0,\Omega} \\
&\lesssim h^2 \Big(\sum_{K\in\Omega_h} ||f||^2_{0,K}\Big)^{1/2} ||v_h||_{0,\Omega} \\
&\lesssim h^2 ||f||_{0,\Omega} ||v_h||_{0,\Omega}.
\end{aligned} \tag{14}$$

Moreover, [22, Theorem 5.1] leads to

$$\sum_{K\in\Omega_h} \Big\{a_{h,K}(w_I^0 - w_\pi^0, v_h) + a_K(w_\pi^0 - w^0, v_h)\Big\} \lesssim h^s ||f||_{0,\Omega} ||v_h||_{2,\Omega}. \tag{15}$$

Thus, by including the estimates (14) and (15) in right-hand side of (13), we get

$$||(\widehat{T}_h - T^0) f||_{0,\Omega} = ||w^0 - w_h||_{0,\Omega} \leq ||w^0 - w_h||_{2,\Omega} \lesssim |w^0 - w_h|_{2,\Omega} \lesssim h^s ||f||_{0,\Omega}. \tag{16}$$

□

On the other hand, we now recall the definitions of the spectral projections E and E_h, associated with pairs (T, μ), and (T_h, μ_h), respectively, which are defined as follows:

$$E := E(\mu) = (2\pi i)^{-1} \int_{\mathcal{C}} (z - T)^{-1} dz, \quad E_h := E_h(\mu_h) = (2\pi i)^{-1} \int_{\mathcal{C}} (z - T_h)^{-1} dz.$$

E and E_h are projections onto the space of generalised eigenvectors $R(E)$ and $R(E_h)$, respectively, where R denotes the range. As a consequence of these definitions, we can

follow the same arguments as those applied to [22, Section 5] to obtain the following results.

Theorem 9 *Given a space $R(E) \subset H^{2+s}(\Omega)$, $s \in (1/2, 1]$, there exists a positive constant h_0 independent of h, such that for all $h < h_0$, we have*

$$\left|\lambda - \lambda_h^{(j)}\right| \lesssim h^{2s}, \qquad j = 1, \dots, m\,. \tag{17a}$$

$$\left|\lambda - \lambda_h^{(j)}\right| \lesssim \left(||u - u_h||_{2,\Omega}^2 + ||u - \Pi_K^0 u_h||_{0,\Omega}^2 + |u - \Pi_K^\Delta u_h|_{2,h}^2\right). \tag{17b}$$

Proof Estimate (17a) was established in [30, Theorem 4.5]. The proof for (17b) can be followed repeating the same arguments as those used in [30, Theorem 4.5], but in this case considering $\Pi_K^\Delta u_h$ instead of w_π and using the fact $\Pi_K^0 v_h = \Pi_K^\Delta v_h$ for all $v_h \in V_h$. □

The following lemma establishes an L^2-norm error estimate for the source problem associated with the operator $\widehat{T}_h$, which will be useful in a posteriori error analysis.

Lemma 10 *For all $f \in R(E)$, if $w = Tf$ and $w_h = \widehat{T}_h f = T_h \mathcal{P}_h f$, then*

$$||w - w_h||_{0,\Omega} \lesssim h^s \left\{|w - w_h|_{2,\Omega} + |w - \Pi_K^\Delta w_h|_{2,h} + ||w - \Pi_K^0 w_h||_{0,\Omega}\right\}.$$

Proof Let $f \in R(E)$, if $w = Tf$ and $w_h = \widehat{T}_h f = T_h \mathcal{P}_h f$, consider $v \in V$ the unique solution of

$$a(v, z) = b(w - w_h, z) \qquad \forall z \in V. \tag{18}$$

From the definition of T, we have that $T(w - w_h) = v$, and using the standard regularity result for the biharmonic problem yields (see eg. [43]) $v \in H^{2+s}(\Omega)$ ($s \in (1/2, 1]$) satisfying

$$||v||_{2+s,\Omega} \lesssim ||w - w_h||_{0,\Omega}. \tag{19}$$

On the other hand, we consider $v_I \in V_h$ as in Proposition 7. Thus, testing the equation (18) with $z \equiv w - w_h \in V$, we have

$$\begin{aligned} ||w - w_h||_{0,\Omega}^2 &= a(w - w_h, v - v_I) + a(w - w_h, v_I) \\ &\lesssim |w - w_h|_{2,\Omega} |v - v_I|_{2,\Omega} + a(w - w_h, v_I) \\ &\lesssim h^s |w - w_h|_{2,\Omega} |v|_{2+s,\Omega} + \Big\{a_h(w_h, v_I) - a(w_h, v_I) \\ &\quad + b(f, v_I) - b_h(\mathcal{P}_h f, v_I)\Big\} \end{aligned}$$

$$\lesssim h^s|w-w_h|_{2,\Omega}||w-w_h||_{0,\Omega}+\Big\{a_h(w_h,v_I)-a(w_h,v_I)+b(f,v_I)-b_h(\mathcal{P}_h f,v_I)\Big\}. \tag{20}$$

Next, note that using the properties of consistence and stability for $a_h(\cdot,\cdot)$, Proposition 7, (19), and [30, Lemma 2.2], we obtain

$$\begin{aligned}
a_h(w_h,v_I)-a(w_h,v_I)&=\sum_{K\in\Omega_h}\Big\{a_{h,K}(w_h-\Pi_K^\Delta w_h,v_I-v_\pi)+a(w_h-\Pi_K^\Delta w_h,v_\pi-v_I)\Big\}\\
&\lesssim\Big\{\sum_{K\in\Omega_h}|w_h-\Pi_K^\Delta w_h|^2_{2,K}\Big\}^{1/2}\Big\{\sum_{K\in\Omega_h}|v_I-v_\pi|^2_{2,K}\Big\}^{1/2}\\
&\le\Big\{\sum_{K\in\Omega_h}|w-w_h|^2_{2,K}+|w-\Pi_K^\Delta w_h|^2_{2,K}\Big\}^{1/2}\Big\{\sum_{K\in\Omega_h}|v-v_I|^2_{2,K}+|v-v_\pi|^2_{2,K}\Big\}^{1/2}\\
&\lesssim h^s\Big\{\sum_{K\in\Omega_h}|w-w_h|^2_{2,K}+|w-\Pi_K^\Delta w_h|^2_{2,K}\Big\}^{1/2}|v|_{2+s,\Omega}\\
&\lesssim h^s\Big\{\sum_{K\in\Omega_h}|w-w_h|^2_{2,K}+|w-\Pi_K^\Delta w_h|^2_{2,K}\Big\}^{1/2}||w-w_h||_{0,\Omega}\\
&\lesssim h^s\Big\{|w-w_h|_{2,\Omega}+|w-\Pi_K^\Delta w_h|_{2,h}\Big\}||w-w_h||_{0,\Omega}.
\end{aligned}\tag{21}$$

Besides, using the fact that $f\in R(E)$, $w=Tf=\mu f$, the definition of $\mathcal{P}_h$, the properties of consistence and stability of $b(\cdot,\cdot)$, (19), and [30, Lemma 2.2], we deduce

$$\begin{aligned}
b(f,v_I)-b_h(\mathcal{P}_h f,v_I)&=b(\mathcal{P}_h f,v_I)-b_h(\mathcal{P}_h f,v_I)=\sum_{K\in\Omega_h}\Big\{b_K(\mathcal{P}_h f,v_I)-b_{h,K}(\mathcal{P}_h f,v_I)\Big\}\\
&=\sum_{K\in\Omega_h}\Big\{b_K(\mathcal{P}_h f-\mu^{-1}\Pi_K^\Delta w_h,v_I-v_\pi)-b_{h,K}(\mathcal{P}_h f-\mu^{-1}\Pi_K^\Delta w_h,v_I-v_\pi)\Big\}\\
&\lesssim\Big\{\sum_{K\in\Omega_h}||\mathcal{P}_h f-\mu^{-1}\Pi_K^\Delta w_h||^2_{0,K}\Big\}^{1/2}\Big\{\sum_{K\in\Omega_h}(||v-v_I||^2_{0,K}+||v-v_\pi||^2_{0,K})\Big\}^{1/2}\\
&\lesssim\Big\{\sum_{K\in\Omega_h}||\mathcal{P}_h f-\mu^{-1}\Pi_K^\Delta w_h||^2_{0,K}\Big\}^{1/2}\Big\{\sum_{K\in\Omega_h}(h^{2(2+s)}||v||^2_{2+s,K}+h^{2(2+s)}||v||^2_{2+s,K})\Big\}^{1/2}\\
&\lesssim h^{2+s}\Big\{\sum_{K\in\Omega_h}||\mathcal{P}_h f-\mu^{-1}\Pi_K^\Delta w_h||^2_{0,K}\Big\}^{1/2}|v|_{2+s,\Omega}\\
&\lesssim h^{2+s}\mu^{-1}\Big\{\sum_{K\in\Omega_h}||\mathcal{P}_h w-\Pi_K^\Delta w_h||^2_{0,K}\Big\}^{1/2}||w-w_h||_{0,\Omega}\\
&\lesssim h^{2+s}\mu^{-1}\Big\{\sum_{K\in\Omega_h}(||w-\mathcal{P}_h w||^2_{0,K}+||w-\Pi_K^\Delta w_h||^2_{0,K})\Big\}^{1/2}||w-w_h||_{0,\Omega}\\
&\lesssim h^{2+s}\Big\{||w-\mathcal{P}_h w||_{0,\Omega}+||w-\Pi_K^\Delta w_h||_{0,\Omega}\Big\}||w-w_h||_{0,\Omega}\\
&\lesssim h^{2+s}\Big\{||w-w_h||_{0,\Omega}+||w-\Pi_K^\Delta w_h||_{0,\Omega}\Big\}||w-w_h||_{0,\Omega}.
\end{aligned}\tag{22}$$

Therefore, inserting the estimates (21) and (22) in (20), and multiplying by $||w - w_h||_{0,\Omega}^{-1}$, we have

$$\begin{aligned} ||w - w_h||_{0,\Omega} &\lesssim h^s \left\{ |w - w_h|_{2,\Omega} + |w - \Pi_K^\Delta w_h|_{2,h} \right\} \\ &\quad + Ch^{2+s} \left\{ ||w - w_h||_{0,\Omega} + ||w - \Pi_K^\Delta w_h||_{0,\Omega} \right\} \\ &\lesssim h^s \left\{ |w - w_h|_{2,\Omega} + |w - \Pi_K^\Delta w_h|_{2,h} + ||w - \Pi_K^\Delta w_h||_{0,\Omega} \right\}. \end{aligned}$$

□

4.1 Error estimates on L^2-norm for the eigenfunctions

In this section, we present an error estimation result for eigenfunctions in the L^2-norm that will be used to demonstrate reliability in a posteriori error estimation. To this end, we first introduce the proof of an auxiliary lemma.

Lemma 11 *Let $(\mu_h^{(j)}, u_h)$ be an eigenpair of $\widehat{T}_h$ with $j = 1, 2, ..., m$ and $||u_h||_{0,\Omega} = 1$. Then, there exist an eigenfunction $u \in L^2(\Omega)$ of T associated to μ, such that*

$$||u - u_h||_{0,\Omega} \lesssim h^s \left\{ |w - w_h|_{2,\Omega} + ||w - \Pi_K^0 w_h||_{0,\Omega} + |w - \Pi_K^\Delta w_h|_{2,h} \right\}. \quad (23)$$

Proof From (12b) and the classical theory for compact operators presented in [6], we know that $sp(\widehat{T}_h)$ converges to $sp(T^0)$. Moreover, from the relation between the eigenfunctions of T and T_h with those of T^0 and $\widehat{T}_h$, respectively, we obtain that $u_h \in R(E_h)$ and there exists $u \in R(E)$ such that

$$||u - u_h||_{0,\Omega} \lesssim \sup_{f^0 \in R(E^0), ||f^0||_{0,\Omega}=1} ||(T^0 - \widehat{T}_h) f^0||_{0,\Omega}.$$

In addition, we have from Lemma 10 that for each $f^0 \in R(E^0)$ satisfying $f^0 = f$ implies

$$||(T^0 - \widehat{T}_h) f^0||_{0,\Omega} = ||(T - \widehat{T}_h) f||_{0,\Omega} \lesssim h^s \left\{ |w - w_h|_{2,\Omega} + |w - \Pi_K^\Delta w_h|_{2,h} + ||w - \Pi_K^\Delta u_h||_{0,\Omega} \right\}.$$

Putting together above inequalities finish the proof. □

Now, we prove the L^2-norm error estimate for the eigenfunctions of the virtual spectral discretization analysed in this work.

Theorem 12 *There exist $s \in (1/2, 1]$ such that*

$$||u - u_h||_{0,\Omega} \lesssim h^s \left\{ |u - u_h|_{2,\Omega} + ||u - \Pi_K^0 u_h||_{0,\Omega} + |u - \Pi_K^\Delta u_h|_{2,h} \right\}.$$

Proof The proof proceeds by bounding each term on the right-hand side of (23) in Lemma 11. We first consider $w \in V$ and $w_h \in V_h$ as the solutions of problems

$$a(w, v) = b(u, v), \quad a_h(w_h, v_h) = b_h(\mathcal{P}_h u, v_h), \quad \forall v \in V, \ \forall v_h \in V_h, \tag{24}$$

respectively. Since $b(u, v) = \frac{1}{\lambda} a(u, v)$ (cf. Problem 1), we get $w = \frac{1}{\lambda} u$ with $\lambda \neq 0$. Thus,

$$|w - w_h|_{2,\Omega} \leq \lambda^{-1} |u - u_h|_{2,\Omega} + |\lambda^{-1} - \lambda_h^{-1}| \, |u_h|_{2,\Omega} + |\lambda_h^{-1} u_h - w_h|_{2,\Omega}. \tag{25}$$

Note that, from estimate (17b), we obtain

$$|\lambda^{-1} - \lambda_h^{-1}| = |\lambda \lambda_h|^{-1} |\lambda - \lambda_h| \lesssim ||u - u_h||_{2,\Omega}^2 + ||u - \Pi_K^0 u_h||_{0,\Omega}^2 + |u - \Pi_K^\Delta u_h|_{2,h}^2. \tag{26}$$

On the other hand, we know that $a_h(\lambda_h^{-1} u_h, v_h) = b_h(u_h, v_h) \ \forall v_h \in V_h$ (cf. Problem 2). Hence, subtracting this equality from (24), we obtain

$$a_h(w_h - \lambda_h^{-1} u_h, v_h) = b_h(\mathcal{P}_h u - u_h, v_h) \ \forall v_h \in V_h.$$

Therefore, using the fact that $a_h(\cdot, \cdot)$ is V_h-elliptic, we can deduce

$$\begin{aligned}
|w_h - \lambda_h^{-1} u_h|_{2,\Omega}^2 &\lesssim a_h(w_h - \lambda_h^{-1} u_h, w_h - \lambda_h^{-1} u_h) \\
&= b_h(\mathcal{P}_h u - u_h, w_h - \lambda_h^{-1} u_h) \\
&\lesssim ||\mathcal{P}_h u - u_h||_{0,\Omega} ||w_h - \lambda_h^{-1} u_h||_{0,\Omega} \\
&\lesssim \left\{ ||\mathcal{P}_h u - u||_{0,\Omega} + ||u - u_h||_{0,\Omega} \right\} ||w_h - \lambda_h^{-1} u_h||_{2,\Omega} \\
&\lesssim \left\{ \inf_{z_h \in V_h} ||u - z_h||_{0,\Omega} + ||u - u_h||_{0,\Omega} \right\} |w_h - \lambda_h^{-1} u_h|_{2,\Omega} \\
&\lesssim ||u - u_h||_{0,\Omega} |w_h - \lambda_h^{-1} u_h|_{2,\Omega} \\
&\lesssim |u - u_h|_{2,\Omega} |w_h - \lambda_h^{-1} u_h|_{2,\Omega}
\end{aligned}$$

which implies that

$$|w_h - \lambda_h^{-1} u_h|_{2,\Omega} \lesssim |u - u_h|_{2,\Omega}. \tag{27}$$

Then, replacing (26) and (27) in the right-hand side of (25) lead to

$$|w - w_h|_{2,\Omega} \lesssim ||u - u_h||_{2,\Omega} + ||u - \Pi_K^0 u_h||_{0,\Omega} + |u - \Pi_K^\Delta u_h|_{2,h}. \tag{28}$$

To bound the second term on the right-hand side of (23), we apply the triangle inequality, and we have

$$||w - \Pi_K^0 w_h||_{0,\Omega} \leq |w - w_h|_{2,\Omega} + ||w_h - \Pi_K^0 w_h||_{0,\Omega}. \tag{29}$$

Next, for the second term in (29), we add and subtract the terms $\lambda_h^{-1}u_h$ and $\lambda_h^{-1}\Pi_K^0 u_h$ to obtain

$$\begin{aligned}||w_h - \Pi_K^0 w_h||_{0,\Omega} &\leq ||w_h - \lambda_h^{-1}u_h||_{0,\Omega} + \lambda_h^{-1}||u_h - \Pi_K^0 u_h||_{0,\Omega} + ||\Pi_K^0(\lambda_h^{-1}u_h - w_h)||_{0,\Omega} \\ &\leq 2|w_h - \lambda_h^{-1}u_h|_{2,\Omega} + \lambda_h^{-1}||u - u_h||_{0,\Omega} + \lambda_h^{-1}||u - \Pi_K^0 u_h||_{0,\Omega} \\ &\lesssim |u - u_h|_{2,\Omega} + ||u - \Pi_K^0 u_h||_{0,\Omega}, \end{aligned} \tag{30}$$

where the boundedness of the projector Π_K^0, the definitions of norms in Sobolev spaces, (27), the triangle inequality and the Poincaré inequality have been used in the last two steps. Thus, replacing (28) and (30) in (29) imply that

$$||w - \Pi_K^0 w_h||_{0,\Omega} \lesssim |u - u_h|_{2,\Omega} + ||u - \Pi_K^0 u_h||_{0,\Omega} + |u - \Pi_K^\Delta u_h|_{2,h}. \tag{31}$$

The third term on the right-hand side of (23) is bounded by following the same arguments as those applied to obtain (31). Therefore,

$$\begin{aligned}|w - \Pi_K^\Delta w_h|_{2,h} &\leq |w - w_h|_{2,\Omega} + |w_h - \Pi_K^\Delta w_h|_{2,h} \\ &= |w - w_h|_{2,\Omega} + \sum_{K\in\Omega_h} |w_h - \Pi_K^\Delta w_h|_{2,K} \\ &\lesssim |u - u_h|_{2,\Omega} + ||u - \Pi_K^0 u_h||_{0,\Omega} + |u - \Pi_K^\Delta u_h|_{2,h}. \end{aligned} \tag{32}$$

Finally, substituting (28), (31) and (32) on the right-hand side of (23) concludes the proof. □

5 A posteriori error analysis

This section is dedicated to constructing a residual-type estimator that depends only on quantities available from the VEM solution, and to establishing its reliability and efficiency. To achieve this, we first present some definitions and local estimates.

To construct a suitable residual-based error estimator, we introduce the jump operator defined as $[\![(\cdot)]\!] := (\cdot)|_K - (\cdot)|_{K'}$, where K and K' are polygons in Ω_h that share a common edge l. Subsequently, the following lemma is stated.

Lemma 13 *For any $v \in V$, the following result is obtained*

$$\begin{aligned}a(u - u_h, v) &= \lambda b(u, v) - \lambda_h b(u_h, v) \\ &\quad + \sum_{K\in\Omega_h} \left\{ a_K(\Pi_K^\Delta u_h - u_h, v) + \lambda_h b_K(u_h - \Pi_K^\Delta u_h, v) \right\} \\ &\quad + \sum_{K\in\Omega_h} \int_K \lambda_h \Pi_K^\Delta u_h v - \sum_{K\in\Omega_h} \sum_{l\in\mathcal{E}_K\cap\mathcal{E}_\Omega} \int_l [\![(\nabla^2 \Pi_K^\Delta u_h)\boldsymbol{n}_K^l]\!] \cdot \nabla v. \end{aligned}$$

Proof Given any $v \in V$ and using the fact that (λ, u) solves the problem (1) and integrating by parts, we readily see that

$$
\begin{aligned}
&a(u-u_h,v) = \lambda b(u,v) - \lambda_h b(u_h,v) + \lambda_h b(u_h,v) - a(u_h,v)\\
&= \lambda b(u,v) - \lambda_h b(u_h,v) + \sum_{K\in\Omega_h}\Big\{a_K(\Pi_K^\Delta u_h - u_h, v) + \lambda_h b_K(u_h,v) - a_K(\Pi_K^\Delta u_h, v)\Big\}\\
&= \lambda b(u,v) - \lambda_h b(u_h,v) + \sum_{K\in\Omega_h}\Big\{a_K(\Pi_K^\Delta u_h - u_h, v) + \lambda_h b_K(u_h - \Pi_K^\Delta u_h, v)\\
&\quad + \lambda_h b_K(\Pi_K^\Delta u_h, v)\Big\} - \sum_{K\in\Omega_h}\left\{\int_{\partial K}\Big[\nabla^2(\Pi_K^\Delta u_h)\boldsymbol{n}_K\Big]\cdot\nabla v - \int_{\partial K} v\Big[\mathrm{div}\nabla^2\Pi_K^\Delta u_h\Big]\cdot\boldsymbol{n}_K\right\}\\
&= \lambda b(u,v) - \lambda_h b(u_h,v) + \sum_{K\in\Omega_h}\Big\{a_K(\Pi_K^\Delta u_h - u_h, v) + \lambda_h b_K(u_h - \Pi_K^\Delta u_h, v)\Big\}\\
&\quad + \sum_{K\in\Omega_h}\int_K \lambda_h \Pi_K^\Delta u_h v - \sum_{K\in\Omega_h}\sum_{l\in\mathcal{E}_K\cap\mathcal{E}_\Omega}\int_l [\![(\nabla^2\Pi_K^\Delta u_h)\boldsymbol{n}_K^l]\!]\cdot\nabla v.
\end{aligned}
$$

□

We define the following local error, volume, jump, and stabilisation estimators for all $K \in \Omega_h$.

$$
\begin{aligned}
\eta_K^2 &:= \Xi_K^2 + \sum_{l\in\mathcal{E}_K\cap\mathcal{E}_\Omega}\mathcal{J}_l^2 + S_K^2,\\
\Xi_K^2 &:= h_K^4 ||\lambda_h\Pi_K^\Delta u_h||_{0,K}^2, \quad \mathcal{J}_l^2 := h_l ||[\![(\nabla^2\Pi_K^\Delta u_h)\boldsymbol{n}_K^l]\!]||_{0,l}^2,\\
S_K^2 &:= s_K^\Delta(u_h - \Pi_K^\Delta u_h, u_h - \Pi_K^\Delta u_h) + s_K^0(u_h - \Pi_K^0 u_h, u_h - \Pi_K^0 u_h).
\end{aligned}
$$

In addition, we note that $\mathcal{J}_l$ is computable only on the basis of the output values of the operators in $\mathbf{D_2}$. Finally, our respective global error, volume, jump, and stabilisation estimators are defined as follows:

$$
\eta^2 := \sum_{K\in\Omega_h}\eta_K^2, \quad \Xi^2 := \sum_{K\in\Omega_h}\Xi_K^2, \quad \mathcal{J}^2 := \sum_{K\in\Omega_h}\sum_{l\in\mathcal{E}_K\cap\mathcal{E}_\Omega}\mathcal{J}_l^2, \quad \text{and} \quad S^2 := \sum_{K\in\Omega_h} S_K^2. \tag{33}
$$

Remark 4 The local volume estimator Ξ_K measures the mass balance error (cf. (1)). Note that for the lowest-case order, the contribution from the left-hand side term $\Delta^2(\Pi_K^\Delta u_h)$ vanishes since $\Pi_K^\Delta u_h \in \mathbb{P}_2$. On the other hand, the local jump estimator $\mathcal{J}_h$ quantifies the discontinuity of the normal component of the discrete Hessian $(\nabla^2\Pi_K^\Delta u_h)\boldsymbol{n}_K$. Finally, the local stabilisation estimator S_K appears naturally from the introduction of polynomial projection operators in the discrete bilinear forms.

5.1 Reliability

The following result is important to establish the reliability of the a posteriori error estimator.

Theorem 14 *The following bound holds*

$$|u-u_h|_{2,\Omega} \lesssim \eta + \frac{\lambda+\lambda_h}{2}||u-u_h||_{0,\Omega}. \tag{34}$$

Proof Let $e = u - u_h \in V$, then there exists $e_I \in V_h$ (cf. Proposition 7) such that

$$|e-e_I|_{t,\Omega} \lesssim h^{s-t}|e|_{s,\Omega}, \quad s=2,3, \quad t=0,1,...,s. \tag{35}$$

From Lemma 13, we have that

$$\begin{aligned}
|u-u_h|^2_{2,\Omega} &= a(e,e-e_I) + a(u,e_I) - a_h(u_h,e_I) + a_h(u_h,e_I) - a(u_h,e_I) \\
&= \lambda b(u,e-e_I) - \lambda_h b(u_h,e-e_I) + a(u,e_I) \\
&\quad - \lambda_h b_h(u_h,e_I) + a_h(u_h,e_I) - a(u_h,e_I) \\
&\quad + \sum_{K\in\Omega_h}\int_K \lambda_h \Pi^\Delta_K u_h (e-e_I) + \sum_{K\in\Omega_h}\sum_{l\in\mathcal{E}_K\cap\mathcal{E}_\Omega}\int_l -[\![(\nabla^2\Pi^\Delta_K u_h)\boldsymbol{n}^l_K]\!]\cdot\nabla(e-e_I) \\
&\quad + \sum_{K\in\Omega_h} a_K(\Pi^\Delta_K u_h - u_h, e-e_I) + \lambda_h \sum_{K\in\Omega_h} b_K(u_h - \Pi^\Delta_K u_h, e-e_I) \\
&= \Big\{\lambda b(u,e) - \lambda_h b(u_h,e)\Big\} + \lambda_h\Big\{b(u_h,e_I) - b_h(u_h,e_I)\Big\} \\
&\quad + \Big\{a_h(u_h,e_I) - a(u_h,e_I)\Big\} + \sum_{j=1}^4 E_j,
\end{aligned} \tag{36}$$

where the terms E_j $(j=1,\dots,4)$ are given by:

$$E_1 := \sum_{K\in\Omega_h} a_K(\Pi^\Delta_K u_h - u_h, e-e_I), \qquad E_2 := \lambda_h \sum_{K\in\Omega_h} b_K(u_h - \Pi^\Delta_K u_h, e-e_I),$$

$$E_3 := \sum_{K\in\Omega_h}\int_K \lambda_h \Pi^\Delta_K u_h (e-e_I), \qquad E_4 := \sum_{K\in\Omega_h}\sum_{l\in\mathcal{E}_K\cap\mathcal{E}_\Omega}\int_l -[\![(\nabla^2\Pi^\Delta_K u_h)\boldsymbol{n}^l_K]\!]\cdot\nabla(e-e_I).$$

Now, let us find upper bounds on each term in (36). In fact, if $(\lambda,u) \neq (0,0)$ is an eigenpair of T with λ a simple eigenvalue, we select $||u||_{0,\Omega} = 1$ so that for each mesh Ω_h, the solution (λ_h, u_h) of the Problem 2 satisfy $||u_h||_{0,\Omega} = 1$ and

$|\lambda - \lambda_h|, |u - u_h|_{2,\Omega} \to 0$. Thus, following [44, Lemma 3.4], we have

$$\begin{aligned}
\lambda b(u,e) - \lambda_h b(u_h,e) &= \lambda ||u||^2_{0,\Omega} - (\lambda + \lambda_h) b(u,u_h) + \lambda_h ||u_h||^2_{0,\Omega} \\
&= (\lambda + \lambda_h) - (\lambda + \lambda_h) b(u,u_h) \\
&= \frac{\lambda + \lambda_h}{2} 2\big\{1 - b(u,u_h)\big\} \\
&= \frac{\lambda + \lambda_h}{2} \big\{b(u,u) - 2b(u,u_h) + b(u_h,u_h)\big\} \\
&= \frac{\lambda + \lambda_h}{2} b(u - u_h, u - u_h) \\
&= \frac{\lambda + \lambda_h}{2} ||e||^2_{0,\Omega} \\
&\lesssim \frac{\lambda + \lambda_h}{2} ||e||_{0,\Omega} |e|_{2,\Omega}. \qquad (37)
\end{aligned}$$

On the other hand, using that $b(\cdot,\cdot)$, $b_{h,K}(\cdot,\cdot)$ are scalar products, Lemma 4, and (35), provide the following bound

$$\begin{aligned}
\lambda_h \Big\{ b(u_h, e_I) - b_h(u_h, e_I) \Big\} &= \lambda_h \sum_{K \in \Omega_h} \Big\{ b_K(u_h, e_I) - b_{h,K}(u_h, e_I) \Big\} \\
&\le |\lambda_h| \sum_{K \in \Omega_h} \Big\{ b_K(u_h - \Pi^\Delta_K u_h, u_h - \Pi^\Delta_K u_h)^{1/2} b_K(e_I, e_I)^{1/2} \\
&\quad + b_{h,K}(u_h - \Pi^\Delta_K u_h, u_h - \Pi^\Delta_K u_h)^{1/2} b_{h,K}(e_I, e_I)^{1/2} \Big\} \\
&\lesssim \Big\{ \sum_{K \in \Omega_h} b_{h,K}(u_h - \Pi^\Delta_K u_h, u_h - \Pi^\Delta_K u_h) \Big\}^{1/2} ||e_I||_{0,\Omega} \\
&\lesssim \Big\{ \sum_{K \in \Omega_h} b_{h,K}(u_h - \Pi^\Delta_K u_h, u_h - \Pi^\Delta_K u_h) \Big\}^{1/2} |e|_{2,\Omega}. \qquad (38)
\end{aligned}$$

Following the same arguments, we obtain

$$a_h(u_h, e_I) - a(u_h, e_I) \lesssim \Big\{ \sum_{K \in \Omega_h} a_K(u_h - \Pi^\Delta_K u_h, u_h - \Pi^\Delta_K u_h) \Big\}^{1/2} |e|_{2,\Omega}. \qquad (39)$$

Next, (35) and Lemma 4 imply that

$$\begin{aligned}
E_1 &\le \sum_{K \in \Omega_h} a_K(u_h - \Pi^\Delta_K u_h, u_h - \Pi^\Delta_K u_h)^{1/2} |e|_{2,K} \\
&= \sum_{K \in \Omega_h} s^\Delta_K(u_h - \Pi^\Delta_K u_h, u_h - \Pi^\Delta_K u_h)^{1/2} |e|_{2,K} \\
&\lesssim \Big(\sum_{K \in \Omega_h} S^2_K \Big)^{1/2} |e|_{2,\Omega}. \qquad (40)
\end{aligned}$$

Similarly, (35) and Lemma 4 lead to

$$E_2 = \sum_{K\in\Omega_h} b_K(\Pi_K^\Delta u_h - u_h, e - e_I) \lesssim \Big(\sum_{K\in\Omega_h} S_K^2\Big)^{1/2} |e|_{2,\Omega}. \tag{41}$$

To bound E_3, we apply the Cauchy-Schwarz inequality and (35) to obtain

$$\begin{aligned} E_3 &\le \sum_{K\in\Omega_h} ||\lambda_h \Pi_K^\Delta u_h||_{0,K} ||e - e_I||_{0,K} \\ &\lesssim \Big(\sum_{K\in\Omega_h} h_K^4 ||\lambda_h \Pi_K^\Delta u_h||_{0,K}^2\Big)^{1/2} |e|_{2,\Omega} \\ &= \Big(\sum_{K\in\Omega_h} \Xi_K^2\Big)^{1/2} |e|_{2,\Omega}. \end{aligned} \tag{42}$$

For E_4, the trace inequality for $\nabla(e - e_I) \in H^1(K)$ and (35) provide that

$$\begin{aligned} E_4 &\le \sum_{K\in\Omega_h} \sum_{l\in\mathcal{E}_K\cap\mathcal{E}_\Omega} \Big|\Big|[\![(\nabla^2 \Pi_K^\Delta u_h)\boldsymbol{n}_K^l]\!]\Big|\Big|_{0,l} ||\nabla(e - e_I)||_{0,l} \\ &\le \sum_{K\in\Omega_h} \sum_{l\in\mathcal{E}_K\cap\mathcal{E}_\Omega} \Big|\Big|[\![(\nabla^2 \Pi_K^\Delta u_h)\boldsymbol{n}_K^l]\!]\Big|\Big|_{0,l} \Big\{h_K^{-1/2} ||\nabla(e - e_I)||_{0,K} + h_K^{1/2} |\nabla(e - e_I)|_{1,K}\Big\} \\ &\le \sum_{K\in\Omega_h} \sum_{l\in\mathcal{E}_K\cap\mathcal{E}_\Omega} h_K^{1/2} \Big|\Big|[\![(\nabla^2 \Pi_K^\Delta u_h)\boldsymbol{n}_K^l]\!]\Big|\Big|_{0,l} ||\nabla e||_{1,K} \\ &\lesssim \Big\{\sum_{K\in\Omega_h} \sum_{l\in\mathcal{E}_K\cap\mathcal{E}_\Omega} h_K \Big|\Big|[\![(\nabla^2 \Pi_K^\Delta u_h)\boldsymbol{n}_K^l]\!]\Big|\Big|_{0,l}^2\Big\}^{1/2} ||\nabla e||_{1,\Omega} \\ &= \Big\{\sum_{K\in\Omega_h} \sum_{l\in\mathcal{E}_K\cap\mathcal{E}_\Omega} \mathcal{J}_l^2\Big\} ||e||_{2,\Omega} \\ &\lesssim \mathcal{J}^2 |e|_{2,\Omega}, \end{aligned} \tag{43}$$

where in the last step, we used the Poincaré inequality.

Finally, the proof finishes by replacing (37)-(43) in (36) and using the Cauchy-Schwarz inequality. □

The following result is a consequence of Theorem 14.

Corollary 15 *The following bound holds*

$$||u - \Pi_K^0 u_h||_{0,\Omega} + |u - \Pi_K^\Delta u_h|_{2,h} \lesssim \eta + \frac{\lambda + \lambda_h}{2} ||u - u_h||_{0,\Omega}.$$

As a consequence, it holds

$$|u - u_h|_{2,\Omega} + ||u - \Pi_K^0 u_h||_{0,\Omega} + |u - \Pi_K^\Delta u_h|_{2,h} \lesssim \eta + \frac{\lambda + \lambda_h}{2} ||u - u_h||_{0,\Omega}.$$

Proof Given any $K \in \Omega_h$, the following bound holds

$$||u - \Pi_K^0 u_h||_{0,K} \lesssim ||u - u_h||_{0,K} + ||u_h - \Pi_K^0 u_h||_{0,K} \lesssim ||u - u_h||_{2,K} + ||u_h - \Pi_K^0 u_h||_{0,K}.$$

Next, by adding $|u - \Pi_K^\Delta u_h|_{2,K}$ in the above inequality and summing for all $K \in \Omega_h$, we have

$$\begin{aligned} ||u - \Pi_K^0 u_h||_{0,\Omega}^2 + |u - \Pi_K^\Delta u_h|_{2,h}^2 &\lesssim ||u - u_h||_{2,\Omega}^2 + \sum_{K\in\Omega_h} \Big\{ |u - \Pi_K^\Delta u_h|_{2,K}^2 + ||u_h \\ &\quad - \Pi_K^0 u_h||_{0,K}^2 \Big\} \\ &\lesssim |u - u_h|_{2,\Omega}^2 + \sum_{K\in\Omega_h} \Big\{ |u - \Pi_K^\Delta u_h|_{2,K}^2 + ||u_h \\ &\quad - \Pi_K^0 u_h||_{0,K}^2 \Big\}. \end{aligned}$$

Finally, the proof is obtained from Lemma 4, the definition of the stabilisation estimator S_K, and Theorem 14. □

Theorem 17 (cf. (17b)) and Corollary 15 provide the following result.

Corollary 16 *The following bound holds*

$$|\lambda - \lambda_h| \lesssim \left\{ \eta + \frac{\lambda + \lambda_h}{2} ||u - u_h||_{0,\Omega} \right\}^2.$$

Notice that the terms on the right-hand side in Corollaries 15 and 16 depend of $||u - u_h||_{0,\Omega}$, which are not computable on the basis provided by the output values of the operators in $\mathbf{D_1}$ and $\mathbf{D_2}$. Therefore, we establish a result showing that the term $||u - u_h||_{0,\Omega}$ is asymptotically negligible.

Theorem 17 *The following bounds hold*

(i) $|u - u_h|_{2,\Omega} + ||u - \Pi_K^0 u_h||_{0,\Omega} + |u - \Pi_K^\Delta u_h|_{2,h} \lesssim \eta.$
(ii) $|\lambda - \lambda_h| \lesssim \eta^2.$

Proof (i) Using the Theorem 12 and Corollary 15, we deduce

$$\begin{aligned} &|u - u_h|_{2,\Omega} + ||u - \Pi_K^0 u_h||_{0,\Omega} + |u - \Pi_K^\Delta u_h|_{2,h} \\ &\lesssim \eta + h^s \Big\{ |u - u_h|_{2,\Omega} + ||u - \Pi_K^0 u_h||_{0,\Omega} + |u - \Pi_K^\Delta u_h|_{2,h} \Big\}. \end{aligned}$$

Therefore, the results clear that there exists $h_0 > 0$ such that $\forall h < h_0$ the item (i) is true.

(ii) Again from Theorem 12 and item (i), we have the existence of $h_0 > 0$ such that for all $h < h_0$ implies

$$||u - u_h||_{0,\Omega} \lesssim h^s \eta, \tag{44}$$

and applying (44) in Corollary 16, we have the result. □

5.2 Efficiency

This section proves that our error estimator η is efficient up to oscillation terms given by the polynomial projections Π^0_K and Π^{Δ}_K. We start by recalling properties of bubble functions in the space $H^2_0(K)$.

Remark 5 Given any polygon $K \in \Omega_h$, consider Ω_h^K its sub-triangulation, which it is well defined from the star-shaped property of K. In addition, as a consequence of the assumptions **(A1)** and **(A2)**, it holds that $\widehat{\Omega}_h := \bigcup_{K\in\Omega_h} \Omega_h^K$ is also a shape-regular family of triangulations of Ω. Therefore, by following the arguments established in [45, Section 3.7], an interior bubble function $\psi_K \in H^2_0(K)$ can be defined piecewise as the sum of interior bubble functions of the form $\varphi_T := \mathrm{b}_T^2$, where $\mathrm{b}_T \in H^1_0(T)$ is the triangle interior bubble function constructed on each triangle T of the mesh element Ω_h^K. In addition, it holds

$$||q_K||^2_{0,K} \lesssim \int_K \psi_K q_K^2, \qquad \forall q_K \in \mathbb{P}_2(K), \tag{45a}$$

$$||\psi_K q_K||_{0,K} \leq ||q_K||_{0,K}, \qquad \forall q_K \in \mathbb{P}_2(K). \tag{45b}$$

Moreover, for any edge $l \in \mathcal{E}$, let $K^+, K^- \in \Omega_h$ be the two polygons sharing l as a common edge. Consider the sub-triangulation $\widehat{\Omega}_h$ of Ω_h, and define $\widehat{\mathcal{E}}^l := \{\widehat{l} \in \widehat{\mathcal{E}} : \widehat{l} \subset l\}$ and $\widehat{\mathcal{E}} := \{\widehat{l} \subset \partial T : T \in \widehat{\Omega}_h\}$. In other words, l is the union of edges in $\widehat{\mathcal{E}}^l$. Moreover, each edge $\widehat{l} \in \widehat{\mathcal{E}}$ is shared by exactly two triangles $T^+, T^- \in \widehat{\Omega}_h$; a bubble function $\psi_l \in H^2_0(l)$ is defined piecewise as the sum of bubble functions of the form $\varphi_{\widehat{l}} := (\mathrm{b}_{T^+} - \mathrm{b}_{T^-})\mathrm{b}_{\widehat{l}}$, where $\mathrm{b}_{\widehat{l}} \in H^1_0(\widehat{l})$ is the edge bubble function. Furthermore, the following holds.

$$h_l^{-1}||q_l||^2_{0,l} \lesssim \int_l q_l \mathbf{n}^l_K \cdot \nabla(\psi_l q_l), \qquad \forall q_l \in \mathbb{P}_0(l), \tag{46a}$$

$$||\mathbf{n}^l_{K^+} \cdot \nabla(\psi_l q_l)||_{0,l} \lesssim h_l^{-1}||q_l||_{0,l}, \qquad \forall q_l \in \mathbb{P}_0(l), \tag{46b}$$

$$\sum_{K=K^+,K^-} h_l^{-2}||\psi_l q_l||_{0,K} \lesssim \sum_{K=K^+,K^-} |\psi_l q_l|_{2,K} \lesssim \sum_{K=K^+,K^-} h_l^{-2}||\psi_l q_l||_{0,K}, \qquad \forall q_l \in \mathbb{P}_0(l), \tag{46c}$$

$$\sum_{K=K^+,K^-} ||\psi_l q_l||_{0,K} \lesssim h_l^{1/2}||q_l||_{0,l}, \qquad \forall q_l \in \mathbb{P}_0(l). \tag{46d}$$

In addition, we recall the local inverse estimates established in [46] for any virtual function

$$|v|_{2,K} \lesssim h_K^{-2}||v||_{0,K}, \quad \forall v \in V_h^K. \tag{47}$$

Now, we are ready to prove the efficiency of the local volume estimator Ξ_K.

Lemma 18 *The following bound holds*

$$\Xi_K \lesssim |u - u_h|_{2,K} + S_K + h_K^2 ||\lambda_h u_h - \lambda u||_{0,K}. \tag{48}$$

Proof Given any $K \in \Omega_h$, consider its respective interior bubble function ψ_K (cf. Remark 5) and define $v^K := \psi_K \lambda_h \Pi_K^\Delta u_h$. Since $v^K = \partial_{\boldsymbol{n}_K} v^K = 0$ on ∂K, we extend v^K by zero in all Ω such that $v^K \in V$. In the rest of the proof, we denote this extension by $v \in V$. Therefore, from Lemma 13, we have

$$\int_K \lambda_h \Pi_K^\Delta u_h v = a_K(e, v) - \Big[\lambda b_K(u, v) - \lambda_h b_K(u_h, v) + \Big\{a_K(\Pi_K^\Delta u_h - u_h, v) + \lambda_h b_K(u_h - \Pi_K^\Delta u_h, v)\Big\}\Big].$$

Next, for $q_K \equiv \lambda_h \Pi_K^\Delta u_h \in \mathbb{P}_2(K)$ in (45a) and identity above, we get

$$\begin{aligned}
||\lambda_h \Pi_K^\Delta u_h||_{0,K}^2 &\lesssim \int_K \psi_K (\lambda_h \Pi_K^\Delta u_h)^2 = \int_K \lambda_h \Pi_K^\Delta u_h v \\
&= a_K(e, v) - \Big[b_K(\lambda u - \lambda_h u_h, v) + \Big\{a_K(\Pi_K^\Delta u_h - u_h, v) + \lambda_h b_K(u_h - \Pi_K^\Delta u_h, v)\Big\}\Big] \\
&\lesssim |e|_{2,K} |v|_{2,K} + ||\lambda u - \lambda_h u_h||_{0,K} ||v||_{0,K} + |\Pi_K^\Delta u_h \\
&\quad - u_h|_{2,K} |v|_{2,K} + ||\Pi_K^\Delta u_h - u_h||_{0,K} ||v||_{0,K}.
\end{aligned} \tag{49}$$

Next, from (45b), we have

$$||v||_{0,K} = ||\psi_K \lambda_h \Pi_K^\Delta u_h||_{0,K} \leq ||\lambda_h \Pi_K^\Delta u_h||_{0,K}. \tag{50}$$

In addition, using $0 \leq \psi_K \leq 1$ and the fact that $\lambda_h \Pi_K^\Delta u_h \in \mathbb{P}_2(K) \subseteq V_h^K$ on (47) to obtain

$$|v|_{2,K} = |\psi_K \lambda_h \Pi_K^\Delta u_h|_{2,K} \lesssim |\lambda_h \Pi_K^\Delta u_h|_{2,K} \lesssim h_K^{-2} ||\lambda_h \Pi_K^\Delta u_h||_{0,K}. \tag{51}$$

Therefore, by inserting (50), (51) in (49), we have

$$\begin{aligned}
||\lambda_h \Pi_K^\Delta u_h||_{0,K}^2 &\lesssim |e|_{2,K} |v|_{2,K} + ||\lambda u - \lambda_h u_h||_{0,K} ||v||_{0,K} + |\Pi_K^\Delta u_h - u_h|_{2,K} |v|_{2,K} \\
&\quad + ||\Pi_K^\Delta u_h - u_h||_{0,K} ||v||_{0,K} \\
&\lesssim \Big(h_K^{-2} |e|_{2,K} + ||\lambda u - \lambda_h u_h||_{0,K} + h_K^{-2} |\Pi_K^\Delta u_h - u_h|_{2,K} \\
&\quad + ||\Pi_K^\Delta u_h - u_h||_{0,K}\Big) ||\lambda_h \Pi_K^\Delta u_h||_{0,K},
\end{aligned} \tag{52}$$

which, together with the fact that $\Pi^0_K u_h = \Pi^\Delta_K u_h$, imply

$$||\lambda_h \Pi^\Delta_K u_h||_{0,K} \lesssim \Big(h_K^{-2}|e|_{2,K} + ||\lambda u - \lambda_h u_h||_{0,K} + h_K^{-2}|\Pi^\Delta_K u_h - u_h|_{2,K} + ||\Pi^0_K u_h - u_h||_{0,K}\Big).$$

Next, using Lemma 4 and definition of the he local stabilisation estimator S_K^2 it follows

$$||\lambda_h \Pi^\Delta_K u_h||_{0,K} \lesssim \Big(h_K^{-2}|e|_{2,K} + ||\lambda u - \lambda_h u_h||_{0,K} + h_K^{-2} S_K + S_K\Big).$$

Finally, multiplying by h_K^2 in the above inequality and using the definitions of Ξ_K, we get

$$\begin{aligned}\Xi_K &= h_K^2 ||\lambda_h \Pi^\Delta_K u_h||_{0,K} \\ &\lesssim \Big(|e|_{2,K} + h_K^2 ||\lambda u - \lambda_h u_h||_{0,K} + S_K + h_K^2 S_K\Big) \\ &\lesssim \Big(|u - u_h|_{2,K} + h_K^2 ||\lambda u - \lambda_h u_h||_{0,K} + S_K\Big).\end{aligned}$$

□

Next, we will show an upper bound for the local stabilisation term S_K and the local jump estimator $\mathcal{J}_l$.

Lemma 19 *The following bound holds*

$$S_K \lesssim |u - u_h|_{2,K} + |u - \Pi^\Delta_K u_h|_{2,K} + ||u - \Pi^0_K u_h||_{0,K}.$$

Proof The definition of the stabilisation term and the Cauchy-Schwarz inequality imply that

$$\begin{aligned}S_K &= a_{h,K}(u_h - \Pi^\Delta_K u_h, u_h - \Pi^\Delta_K u_h)^{1/2} + b_{h,K}(u_h - \Pi^\Delta_K u_h, u_h - \Pi^\Delta_K u_h)^{1/2} \\ &\lesssim a_K(u_h - \Pi^\Delta_K u_h, u_h - \Pi^\Delta_K u_h)^{1/2} + b_K(u_h - \Pi^\Delta_K u_h, u_h - \Pi^\Delta_K u_h)^{1/2} \\ &\lesssim |u_h - \Pi^\Delta_K u_h|_{2,K} + ||u - \Pi^0_K u_h||_{0,K} \\ &\lesssim |u - u_h|_{2,K} + |u - \Pi^\Delta_K u_h|_{2,K} + ||u - \Pi^0_K u_h||_{0,K}.\end{aligned}$$

□

Lemma 20 *Let* $\omega(l) := \Big\{K' \in \Omega_h : l \in \partial K'\}$. *Then, the following bound holds*

$$\mathcal{J}_l \lesssim \sum_{K' \in \omega(l)} \Big\{|u - u_h|_{2,K'} + h_{K'}^2 ||\lambda u - \lambda_h u_h||_{0,K'} + S_{K'}\Big\}, \quad \forall l \in \mathcal{E}_K \cap \mathcal{E}_\Omega. \quad (53)$$

Proof Given any edge $l \in \mathcal{E}$. Let us define ψ_l as the corresponding edge bubble function (cf. Remark 5), and $\hat{v} := \psi_l [\![((\nabla^2 \Pi^\Delta_K u_h)\boldsymbol{n}^l_K) \cdot \boldsymbol{n}^l_K]\!] \in H_0^2(T^+ \cup T^-) \subset V$. Since $\hat{v}$ is a polynomial function, $\hat{v}$ can be extended to $K^+ \cup K^-$, where K^+, $K^- \in \Omega_h$ have l as a common edge. For simplicity, we denote this extension by $\hat{v}$.

Following [47], we consider the identity

$$\|[\![(\nabla^2\Pi_K^\Delta u_h)\boldsymbol{n}_K^l]\!]\|_{0,l} = \|[\![(\nabla^2\Pi_K^\Delta u_h)\boldsymbol{n}_K^l)\cdot\boldsymbol{n}_K^l]\!]\|_{0,l} + \|[\![((\nabla^2\Pi_K^\Delta u_h)\boldsymbol{n}_K^l)\cdot\boldsymbol{t}_K^l]\!]\|_{0,l}, \tag{54}$$

where $\boldsymbol{t}_K^l$ is the tangential counterclockwise vectors of l with respect to ∂K. An inverse inequality ([47]) and given that $\nabla v_h|_{\partial K} \in C^0(\partial K)^2$ for all $K \in \Omega_h$ (cf. Section 3) imply that

$$\|[\![((\nabla^2\Pi_K^\Delta u_h)\boldsymbol{n}_K^l)\cdot\boldsymbol{t}_K^l]\!]\|_{0,l} \lesssim h_l^{-1/2}\|[\![\nabla\Pi_K^\Delta u_h]\!]\|_{0,l} \leq 0. \tag{55}$$

Since $\hat{v} \in H_0^2(T^+ \cup T^-) \subset V$, we readily see that

$$\int_l [\![(\nabla^2\Pi_K^\Delta u_h)\boldsymbol{n}_K^l)\cdot\boldsymbol{n}_K^l]\!](\mathbf{n}_K^l\cdot\nabla\hat{v}) = \int_l [\![(\nabla^2\Pi_K^\Delta u_h)\boldsymbol{n}_K^l]\!]\cdot\nabla\hat{v}. \tag{56}$$

Putting together (46a), (54)-(56), and Lemma 13, we arrive at

$$\begin{aligned}
||[\![(\nabla^2\Pi_K^\Delta u_h)\boldsymbol{n}_K^l]\!]||_{0,l}^2 &\lesssim \int_l [\![(\nabla^2\Pi_K^\Delta u_h)\boldsymbol{n}_K^l]\!]\cdot\nabla\hat{v} \\
&= \sum_{K=T^+,T^-}\Big\{a_K(-e,\hat{v}) + \Big\{\lambda b_K(u,\hat{v}) - \lambda_h b_K(u_h,\hat{v})\Big\} + \sum_{K'\in\omega_l} a_K(\Pi_K^\Delta u_h - u_h,\hat{v}) \\
&\quad + \lambda_h b_K(u_h - \Pi_K^0 u_h,\hat{v}) + \int_K \lambda_h\Pi_K^\Delta u_h\hat{v}\Big\} \\
&\lesssim \sum_{K=T^+,T^-}\Big\{|e|_{2,K}|\hat{v}|_{2,K} + ||\lambda u - \lambda_h u_h||_{0,K}||\hat{v}||_{0,K} + |u_h - \Pi_K^\Delta u_h|_{2,K}|\hat{v}|_{2,K} \\
&\quad + ||u_h - \Pi_K^0 u_h||_{0,K}||\hat{v}||_{0,K} + ||\lambda_h\Pi_K^\Delta u_h||_{0,K}||\hat{v}||_{0,K}\Big\} \\
&\lesssim \sum_{K=T^+,T^-}\Big\{\Big(h_K^{-2}|e|_{2,K} + ||\lambda u - \lambda_h u_h||_{0,K} + h_K^{-2}|u_h - \Pi_K^\Delta u_h|_{2,K} \\
&\quad + ||u_h - \Pi_K^0 u_h||_{0,K} + ||\lambda_h\Pi_K^\Delta u_h||_{0,K}\Big)||\hat{v}||_{0,K}\Big\} \\
&\lesssim \sum_{K=T^+,T^-}\Big\{\Big(h_K^{-1/2}|e|_{2,K} + h_K^{3/2}||\lambda u - \lambda_h u_h||_{0,K} + h_K^{-1/2}|u_h - \Pi_K^\Delta u_h|_{2,K} \\
&\quad + h_K^{3/2}||u_h - \Pi_K^0 u_h||_{0,K} + h_K^{3/2}||\lambda_h\Pi_K^\Delta u_h||_{0,K}\Big)||[\![(\nabla^2\Pi_K^\Delta u_h)\boldsymbol{n}_K^l]\!]||_{0,l}\Big\},
\end{aligned}$$

where $e = u - u_h$ and (46b)-(46c) have been used (respectively) in the fourth and fifth steps. Finally, Lemma 4, the definition of S_K together with Lemma 18, conclude the proof. □

The efficiency of η_K is provided next.

Theorem 21 *The following bound holds*

$$\eta_K^2 \lesssim \sum_{K' \in \omega_K} \left\{ |u - u_h|_{2,K'}^2 + ||u - \Pi_{K'}^0 u_h||_{0,K'}^2 + |u - \Pi_{K'}^{\Delta} u_h|_{2,K'}^2 + h^4 ||\lambda u - \lambda_h u_h||_{0,K'}^2 \right\}$$

Proof The result is obtained from Lemmas 18-20. □

Finally, the term $h_K^2 ||\lambda u - \lambda_h u_h||_{0,K'}$ is asymptotically negligible for the global estimator η, this result is provided below.

Corollary 22 *The following bound holds*

$$\eta^2 \lesssim |u - u_h|_{2,\Omega}^2 + ||u - \Pi_K^0 u_h||_{0,\Omega}^2 + |u - \Pi_K^{\Delta} u_h|_{2,h}^2.$$

Proof The proof follows as in [42, Corollary 5.14]. □

Remark 6 We refer the reader to [17] for more details about the construction of the C^1 virtual element discretisation in 3D. Note that Lemma 13 includes a boundary term (c.f. the jump estimator $\mathcal{J}$ in (33)), which in this case is defined over the faces of each polyhedron. Since this term does not require the explicit evaluation of u_h on the faces–where it belongs to a virtual space–the previously given proofs remain valid in the three-dimensional setting. We refer to [35] for the construction of bubble functions in H_0^1 on faces and polyhedra in the context of virtual element methods; the same ideas can be extended to H_0^2 bubble functions by employing the cut-off functions discussed in [48].

6 Numerical examples

In this section, we present some numerical results that illustrate the properties of the estimator introduced in Section 5, showing the optimal behaviour of the associated adaptive algorithm under different convex polygonal meshes, see Fig. 1. Then, we introduce the classical L-shape domain to illustrate the capability of capturing singularities in non-convex domains.

The numerical implementation is done with the library `VEM++` [40] where the VE space presented in Section 3 is available. To solve the generalised eigenvalues problem arising from such discretisations, `VEM++` contains a wrapper of the C++ library `SLEPC` [49] with the problem type option `EPS-GHEP`. Regarding the adaptive algorithm, we follow the usual strategy

$$\text{SOLVE} \rightarrow \text{ESTIMATE} \rightarrow \text{MARK} \rightarrow \text{REFINE}$$

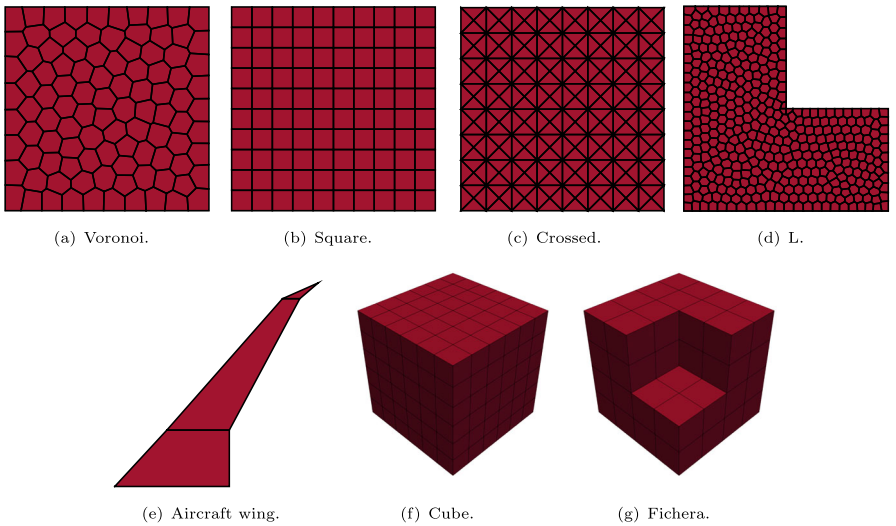

(a) Voronoi. (b) Square. (c) Crossed. (d) L.

(e) Aircraft wing. (f) Cube. (g) Fichera.

Fig. 1 Domain discretisations used for the numerical examples

where the SOLVE and ESTIMATE steps are performed inside `VEM++` using `SLEPC` as a solver for the linear system, in this way, we exploit the high-speed computation capabilities of C++. Next, for the 2D REFINE step, we use the Matlab-based method from [50], which connects edge mid-points to the polygon barycenter. On the other hand, the 3D adaptive refinement routine operates on cubical meshes with support for hanging nodes, making use of the `p4est` library [51] via the `GridapP4est` module of the Julia package `Gridap` [52]. We recall that the refinement procedure is independent of the `VEM++` capabilities. Therefore, the implementation presented in this paper can be extended to more general (non-convex) polygonal shapes that satisfy **A1**, **A2** by selecting an appropriate refinement routine. Finally, for the MARK procedure, we follow a Dörfler/Bulk marking strategy, marking the subset of mesh elements $\mathcal{K} \subseteq \Omega_h$ with the largest estimated errors such that for $\delta = \frac{1}{2} \in [0, 1]$, we have

$$\delta \sum_{K \in \Omega_h} \eta_K^2 \leq \sum_{K \in \mathcal{K}} \eta_K^2.$$

The experimental order of convergence $r(*)$ against the total number of degrees of freedom #DoFs applied to either the error $|\lambda_{i,h} - \lambda_i|$ or the estimator η, and the effectivity index eff of the refinement $1 \leq j$ for $d = 2, 3$ are computed as $r(*)_{j+1} = -d \log\left(*_{j+1}/*_j\right) / \log\left(\#\text{DoFs}_{j+1}/\#\text{DoFs}_j\right)$, $\text{eff}_j = \eta_j^2/|\lambda_{i,h} - \lambda_i|_j$.

6.1 Example 1: Behaviour under uniform refinement: 2D case.

We consider the vibration problem (1) with boundary clamped boundary conditions as in (3) for the unit square $\Omega = (0, 1)^2$ under a variety of discretisations (see Fig. 1a-1c). It is well known that the lowest eigenvalue of this problem is given by $\lambda_1 \approx$

1294.93397959171 (see e.g. [53, 54]). In addition, the associated eigenfunction u_1 is a smooth function, which will not affect the convergence rate.

The curves for the error $|\lambda_{1,h} - \lambda_1|$, and global error estimator η^2 under uniform refinement are shown in Fig. 2. Note that the error is bounded above by the estimator, confirming the reliability of the method (see Theorem 17). In addition, we observe the expected convergence rate of $O(h^2)$ given in (17a). Finally, the effectivity index eff remains bounded for each mesh tested accordingly to Corollary 22.

6.2 Example 2: The role of the stabilisation.

For this numerical experiment, we focus on the vibration problem (1) where $\Omega = (0, 1)^2$, and we consider simply supported boundary conditions (3). Notably, this boundary condition does not alter the discrete formulation presented in Section 3. The main difference is that the linear system incorporates the degrees of freedom corresponding to $\partial_{\boldsymbol{n}} u$. A key advantage of this example is that the first eigenvalue is known explicitly, given by $\lambda_1 = 4\pi^4 \approx 389.6364$ (see [55]). So we can compute the exact error $|\lambda_{1,h} - \lambda_1|$.

Here, we analyse the influence of the stabilisation operator by introducing two coefficients α_Δ, α_0 in the stabilisation term (see [30]) as follows:

$$\alpha_\Delta s_K^\Delta(u_h - \Pi_K^\Delta u_h, u_h - \Pi_K^\Delta u_h), \quad \alpha_0 s_K^0(u_h - \Pi_K^\Delta u_h, u_h - \Pi_K^\Delta u_h).$$

These coefficients appear both in the discrete weak formulation (see Problem 2) and the global stabilisation estimator S. For simplicity, we fix the Voronoi mesh shown in Fig. 1a

In Figs. 3 and 4, we report the curves for the error $|\lambda_{1,h} - \lambda_1|$ and global error estimator η^2 (respectively) for the lowest eigenvalue λ_1 computed by the method for different values of α under uniform refinement. We observe that the SLEPC solver successfully computes an eigenvalue for each uniform refinement and every proposed value of α. However, the results indicate that for the values $\alpha = 1/64$ and $\alpha =$

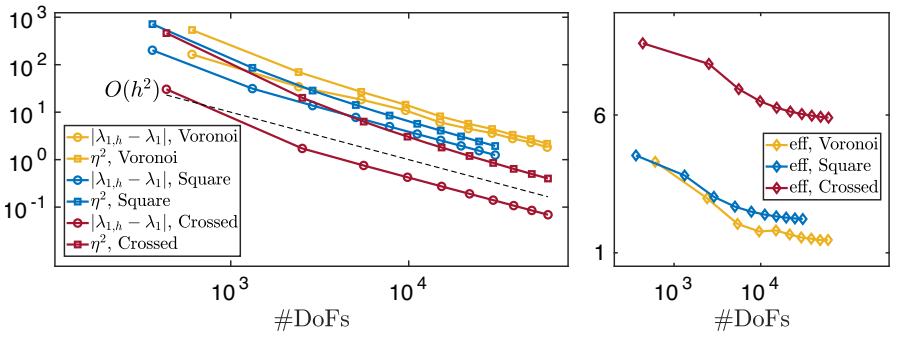

Fig. 2 Example 1. Behaviour of the error $|\lambda_{1,h} - \lambda_1|$, global error estimator η (left), and effectivity index eff (right) for the first eigenvalue λ_1 across various meshes under uniform refinement

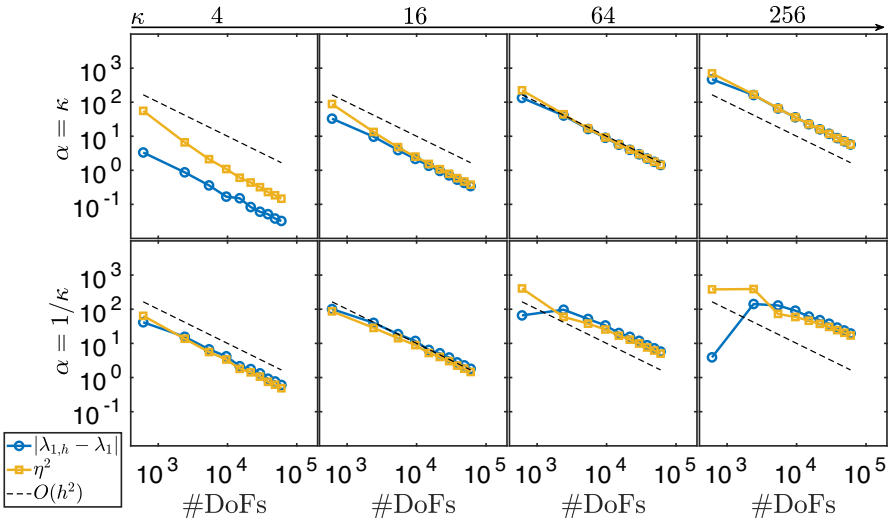

Fig. 3 Example 2. Curves of error $|\lambda_{1,h} - \lambda_1|$, and global error estimator η for the first eigenvalue λ_1 in the Voronoi mesh under uniform refinement with a variation of the stabilisation parameter α

$1/256$, the expected convergence rate of $O(h^2)$ deteriorates due to the influence of this parameter. This observation allows us to extend the results in [30] to the minimal risk interval $\alpha \in [1/64, 256]$, noting that more refinements are required to improve the accuracy of the eigenvalue computed for high values of α.

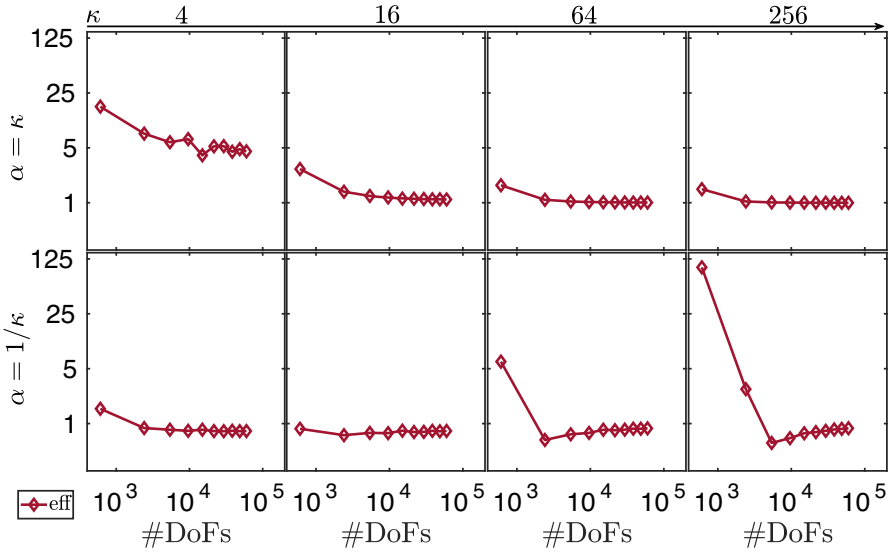

Fig. 4 Example 2. Curves of effectivity index eff for the first eigenvalue λ_1 in the Voronoi mesh under uniform refinement with a variation of the stabilisation parameter α

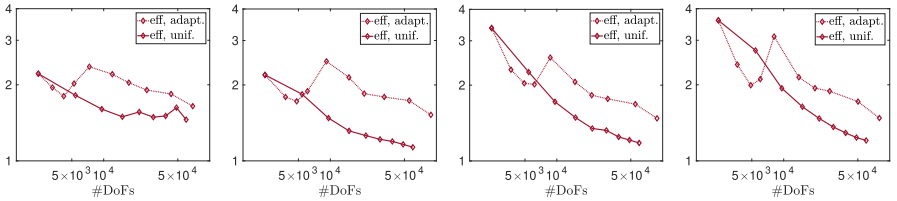

Fig. 5 Example 3. Curves of effectivity index eff for the first four eigenvalues λ_i on the L-shaped domain under adaptive and uniform refinement

6.3 Example 3: Adaptivity in 2D.

In this test, we study the vibration problem (1) defined in the classical L-shape domain given by $\Omega = (0, 1)^2 \setminus (1/2, 1)^2$ with clamped boundary conditions (3). The domain is discretised with a Voronoi-type mesh (see Fig. 1d). It is well known that the first

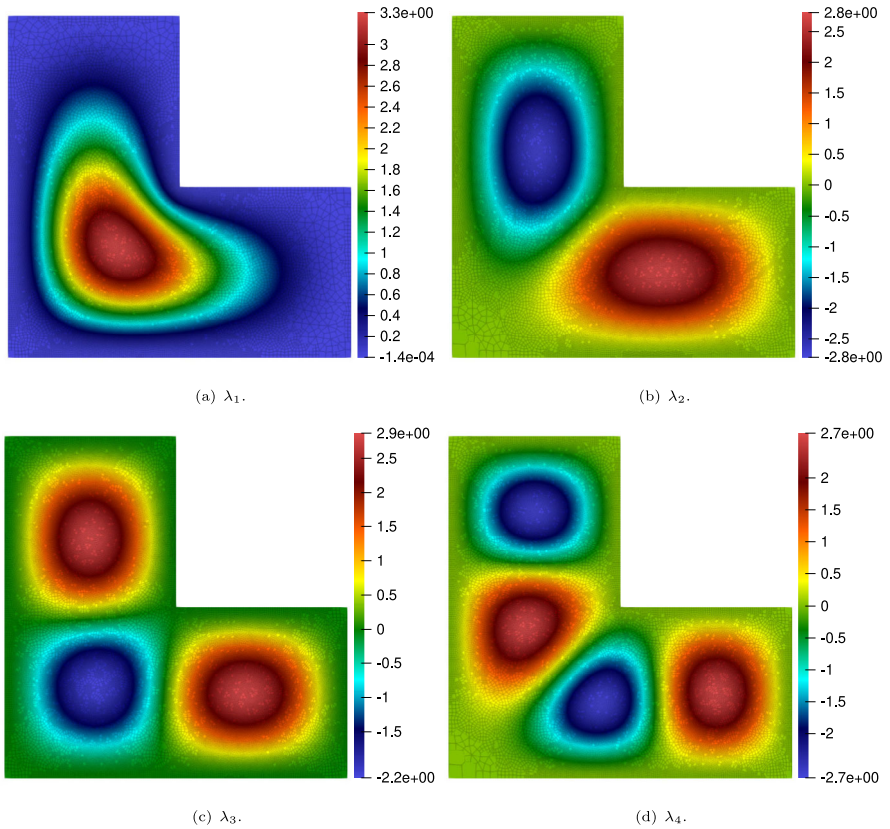

Fig. 6 Example 3. Snapshots of the eigenfunction u_i in the L-shaped mesh for distinct eigenvalues λ_i after 9 refinement steps driven by η

four eigenvalues are given by $\lambda_1 \approx 6704.2982$, $\lambda_2 \approx 11055.5189$, $\lambda_3 \approx 14907.0816$, and $\lambda_4 \approx 26157.9673$ (see e.g. [12, 30]).

Figure 7 reports the convergence history of the method for the error $|\lambda_{i,h} - \lambda_i|$ ($i \in \{1, 2, 3, 4\}$), and the estimator η under adaptive and uniform refinement. We observe that the adaptive refinement outperforms the uniform refinement in the presence of a singularity in the solution, expected by the re-entry corner of the L-shaped domain. Moreover, the effectivity index eff remains bounded between 1 and 4 (see Fig. 5), confirming the efficiency and reliability of the method. Finally, Fig. 6 shows snapshots of the eigenfunctions u_i after 9 adaptive refinement steps driven by η (Fig. 7).

6.4 Example 4: Vibration on an aircraft wing.

As an application, we consider (1) defined in a 2D simplification of an aircraft wing embedded in the unit square whose geometry is shown in Fig. 1e

The initial mesh considered on the adaptive refinement routine is constructed by applying four iterations of polymesher's uniform refinement to the mesh shown in Fig. 1e

The computable global error estimator η^2 is reported in Fig. 8, showing the optimal behaviour of $O(h^2)$ given by Corollary 22. Since exact values of $\lambda_i, i \in \{1, 2, 3, 4\}$ are not provided, we can not compute the error $|\lambda_{i,h} - \lambda_i|$. However, previous examples have already confirmed that the estimator gives an upper bound of this error. The associated eigenfunctions u_i are shown in Fig. 9 after 9 refinement steps driven by η.

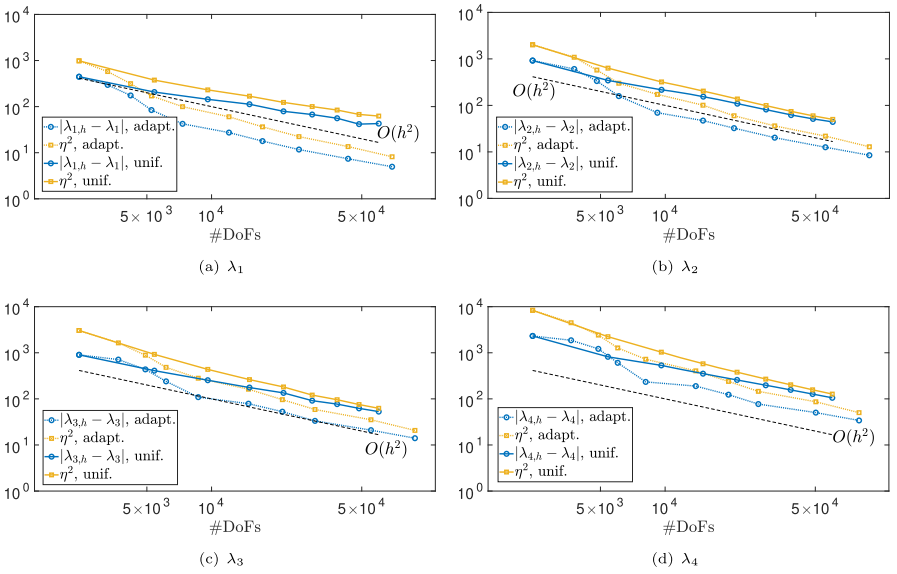

Fig. 7 Example 3. Curves of error $|\lambda_{i,h} - \lambda_i|$ and global error estimator η for the first four eigenvalues λ_i on the L-shaped domain under adaptive and uniform refinement

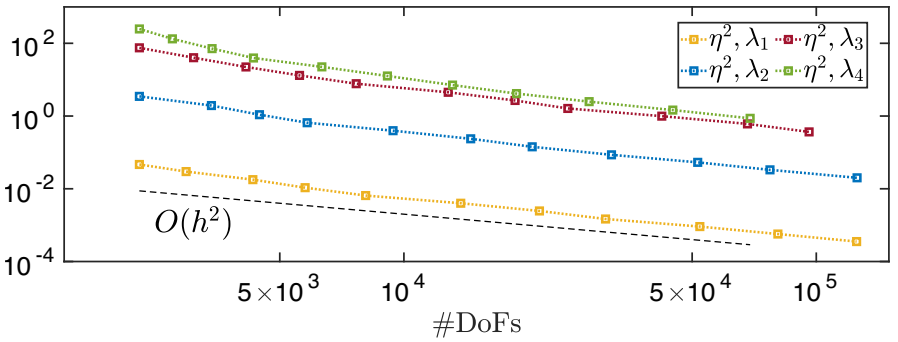

Fig. 8 Example 4. Behaviour of the global error estimator η for the first four eigenvalues λ_i on the aircraft wing

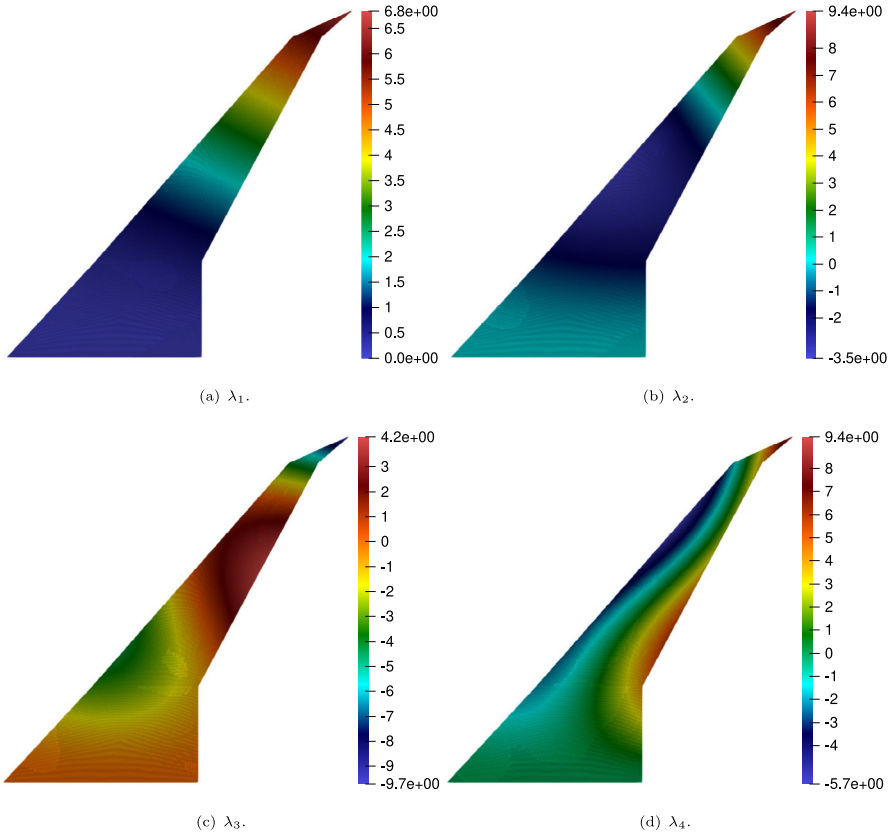

(a) λ_1. (b) λ_2.

(c) λ_3. (d) λ_4.

Fig. 9 Example 4. Snapshots of the eigenfunction u_i in the aircraft wing mesh for distinct eigenvalues λ_i after 9 refinement steps driven by η

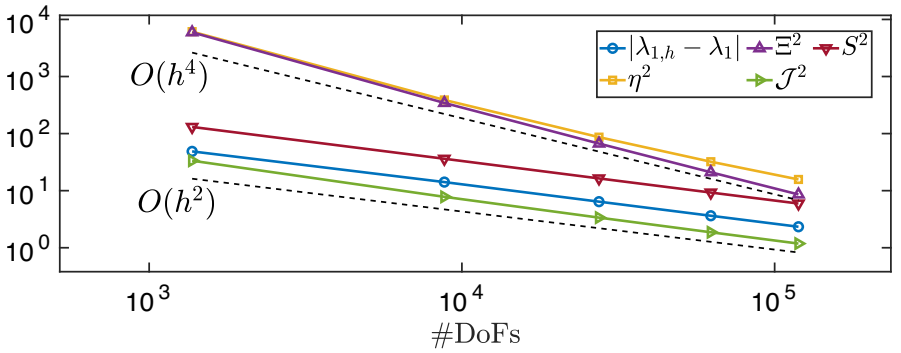

Fig. 10 Example 5. Curves of error $|\lambda_{1,h} - \lambda_1|$, global error η, volume Ξ, jump $\mathcal{J}$, and stabilisation S estimators for the first eigenvalue λ_1 in the unit cube under uniform refinement

6.5 Example 5: Behaviour under uniform refinement: 3D case

This numerical experiment extends Subsection 6.2 to the three-dimensional case. The vibration problem (1) with simply supported boundary conditions (2) is now defined on the unit cube domain $\Omega = (0, 1)^3$ given in Fig. 1f

Due to high computational effort, we were not able to capture the $O(h^2)$ trend. Then, we decided to split the estimator contributions. This analysis is reported in Fig. 10, where we observe that the global volume estimator Ξ with convergence rate of $O(h^4)$ dominates over the global stabilisation estimator S with lower convergence rate of $O(h^2)$. However, the trend shows that S becomes dominant as the uniform refinement progresses while bounding the error $|\lambda_{1,h} - \lambda_1|$. This confirms the reliability of the scheme in the 3D case with the optimal convergence rate.

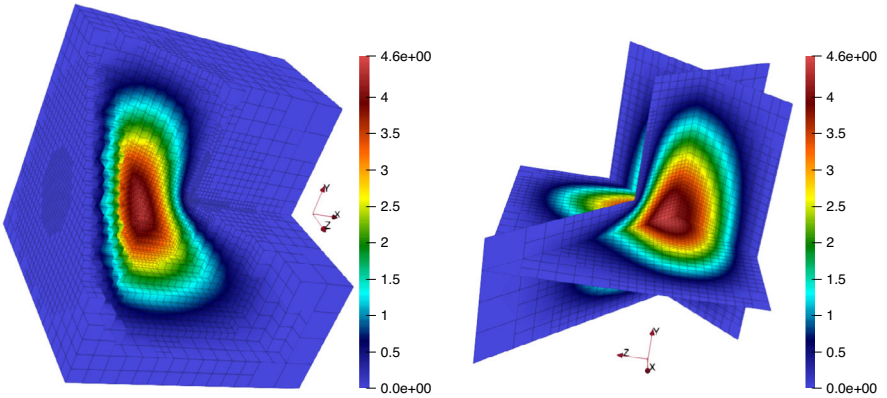

Fig. 11 Example 6. Snapshots of the approximated eigenfunction $u_{1,h}$ in the Fichera cube after 14 adaptive refinement

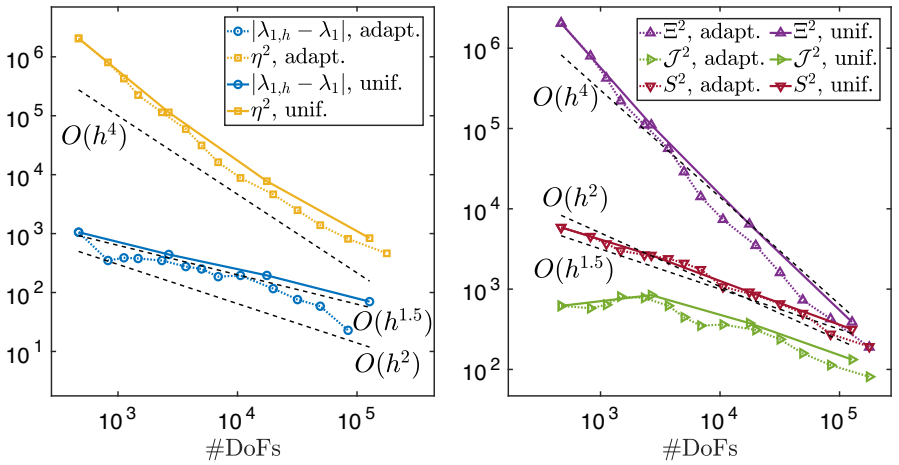

Fig. 12 Example 6. Curves of error $|\lambda_{1,h} - \lambda_1|$, global error η (left), volume Ξ, jump $\mathcal{J}$, and stabilisation S (right) estimators for the first eigenvalue λ_1 in the Fichera cube under uniform and adaptive refinement

6.6 Example 6: Adaptivity in 3D.

To illustrate the applicability of the method in 3D, we consider the vibration problem (1) with clamped boundary conditions (3) in the Fichera cube domain $\Omega = (0, 1)^3 \setminus (1/2, 1)^3$ (see Fig. 1g). We obtain an approximation for the first eigenvalue $\lambda_1 \approx 6657.574172648315$ after 13 adaptive refinement steps. The closest approximation of this value is given in [22]. Similarly to Subsection 6.5, we select $\alpha_\Delta = 1$ and $\alpha_0 = 10^{-4}$ (Fig. 11).

The curves for the error $|\lambda_{1,h} - \lambda_1|$ and global error estimator η are shown in Fig. 12. Note that the adaptive refinement outperforms the uniform refinement, recovering the optimal convergence rate of $O(h^2)$. Moreover, the adaptive refinement captures the singularity of the solution close to the re-entrant corner as shown in Fig. 11.

Acknowledgements We kindly thank Prof. Jesus Vellojin for the support provided in the SLEPC solver implementation.

Author contribution AER and IV designed the methodology. FD and AER developed the code. AER performed the experiments. AER and IV wrote the manuscript. All authors reviewed and approved the final version of the manuscript.

Funding Open Access funding provided by Colombia Consortium. FD was partially supported by the European Research Council project NEMESIS (Grant No. 101115663). AER has been partially supported by the Australian Research Council through the FUTURE FELLOWSHIP grant FT220100496. IV was partially financially supported by Vicerrectoría de la Investigación de la Universidad Militar Nueva Granada (grant INV-CIAS-4167), and this paper is a "Producto derivado del proyecto INV-CIAS-4167 financiado por la Universidad Militar Nueva Granada - Vigencia (2025)."

Declarations

Conflict of interest The authors declare no competing interests.

Open Access This article is licensed under a Creative Commons Attribution 4.0 International License, which permits use, sharing, adaptation, distribution and reproduction in any medium or format, as long as you give appropriate credit to the original author(s) and the source, provide a link to the Creative Commons licence, and indicate if changes were made. The images or other third party material in this article are included in the article's Creative Commons licence, unless indicated otherwise in a credit line to the material. If material is not included in the article's Creative Commons licence and your intended use is not permitted by statutory regulation or exceeds the permitted use, you will need to obtain permission directly from the copyright holder. To view a copy of this licence, visit http://creativecommons.org/licenses/by/4.0/.

References

1. Gazzola, F., Grunau, H.-C., Sweers, G.: Polyharmonic Boundary Value Problems: Positivity Preserving and Nonlinear Higher Order Elliptic Equations in Bounded Domains, 1st edn. Springer Science & Business Media, Berlin, Heidelberg (2010). https://doi.org/10.1007/978-3-642-12245-3
2. Bermúdez, A., Durán, R., Muschietti, M.A., Rodríguez, R., Solomin, J.: Finite element vibration analysis of fluid–solid systems without spurious modes. SIAM J. Numer. Anal. **32**(4), 1280–1295 (1995). https://doi.org/10.1137/0732059
3. Boffi, D.: Finite element approximation of eigenvalue problems. Acta Numer **19**, 1–120 (2010). https://doi.org/10.1017/S0962492910000012
4. Boffi, D., Gardini, F., Gastaldi, L.: In: Blowey, J., Jensen, M. (eds.) Some Remarks on Eigenvalue Approximation by Finite Elements, pp. 1–77. Springer, Berlin, Heidelberg (2012). https://doi.org/10.1007/978-3-642-23914-4_1
5. Ciarlet, P.G.: The Finite Element Method for Elliptic Problems. Classics in Applied Mathematics, vol. 40. Society for Industrial and Applied Mathematics (SIAM), Philadelphia, PA (2002).https://doi.org/10.1137/1.9780898719208
6. Babuška, I., Osborn, J.: Eigenvalue problems. In: Finite Element Methods (Part 1). Handbook of Numerical Analysis, vol. 2, pp. 641–787. Elsevier, Amsterdam, Netherlands (1991). https://doi.org/10.1016/S1570-8659(05)80042-0
7. Rannacher, R.: Nonconforming finite element methods for eigenvalue problems in linear plate theory. Numer. Math. **33**(1), 23–42 (1979). https://doi.org/10.1007/BF01396493
8. Engel, G., Garikipati, K., Hughes, T.J.R., Larson, M.G., Mazzei, L., Taylor, R.L.: Continuous/discontinuous finite element approximations of fourth-order elliptic problems in structural and continuum mechanics with applications to thin beams and plates, and strain gradient elasticity. Comput. Methods Appl. Mech. Engrg. **191**(34), 3669–3750 (2002). https://doi.org/10.1016/S0045-7825(02)00286-4
9. Giani, S.: Solving elliptic eigenvalue problems on polygonal meshes using discontinuous Galerkin composite finite element methods. Appl. Math. Comput. **267**, 618–631 (2015). https://doi.org/10.1016/j.amc.2015.01.011. The Fourth European Seminar on Computing (ESCO 2014)
10. Ciarlet, P.G., Raviart, P.A.: A mixed finite element method for the biharmonic equation. In: de Boor, C. (ed.) Mathematical Aspects of Finite Elements in Partial Differential Equations, pp. 125–145. Academic Press, New York, NY (1974). https://doi.org/10.1016/B978-0-12-208350-1.50009-1
11. Monk, P.: A mixed finite element method for the biharmonic equation. SIAM J. Numer. Anal. **24**(4), 737–749 (1987). https://doi.org/10.1137/0724048
12. Mora, D., Rodríguez, R.: A piecewise linear finite element method for the buckling and the vibration problems of thin plates. Math. Comp. **78**(268), 1891–1917 (2009). https://doi.org/10.1090/S0025-5718-09-02228-5
13. Beirão da Veiga, L., Brezzi, F., Cangiani, A., Manzini, G., Marini, L.D., Russo, A.: Basic principles of virtual element methods. Math. Models Methods Appl. Sci. **23**(1), 199–214 (2013). https://doi.org/10.1142/S0218202512500492
14. Beirão da Veiga, L., Brezzi, F., Marini, L.D., Russo, A.: The hitchhiker's guide to the virtual element method. Math. Models Methods Appl. Sci. **24**(8), 1541–1573 (2014). https://doi.org/10.1142/S021820251440003X
15. Beirão da Veiga, L., Manzini, G.: A virtual element method with arbitrary regularity. IMA J. Numer. Anal. **34**(2), 759–781 (2014). https://doi.org/10.1093/imanum/drt018

16. Antonietti, P.F., Veiga, L.B., Scacchi, S., Verani, M.: A C^1 virtual element method for the Cahn-Hilliard equation with polygonal meshes. SIAM J. Numer. Anal. **54**(1), 34–56 (2016). https://doi.org/10.1137/15M1008117
17. Beirão da Veiga, L., Dassi, F., Russo, A.: A C^1 virtual element method on polyhedral meshes **79**(7), 1936–1955 (2020). https://doi.org/10.1016/j.camwa.2019.06.019. Advanced Computational methods for PDEs
18. Brezzi, F., Marini, L.D.: Virtual element methods for plate bending problems. Comput. Methods Appl. Mech. Engrg. **253**, 455–462 (2013). https://doi.org/10.1016/j.cma.2012.09.012
19. Mora, D., Reales, C., Silgado, A.: A C^1-virtual element method of high order for the brinkman equations in stream function formulation with pressure recovery. IMA J. Numer. Anal. **42**(4), 3632–3674 (2021). https://doi.org/10.1093/imanum/drab078
20. Mora, D., Silgado, A.: A C^1 virtual element method for the stationary quasi-geostrophic equations of the ocean. Comput. Math. Appl. **116**, 212–228 (2022). https://doi.org/10.1016/j.camwa.2021.05.022. New trends in Computational Methods for PDEs
21. Čertík, O., Gardini, F., Manzini, G., Vacca, G.: The virtual element method for eigenvalue problems with potential terms on polytopic meshes. Appl. Math. **63**(3), 333–365 (2018). https://doi.org/10.21136/am.2018.0093-18
22. Dassi, F., Velásquez, I.: Virtual element method on polyhedral meshes for bi-harmonic eigenvalues problems. Comput. Math. Appl. **121**, 85–101 (2022). https://doi.org/10.1016/j.camwa.2022.07.001
23. Gardini, F., Vacca, G.: Virtual element method for second-order elliptic eigenvalue problems. IMA J. Numer. Anal. **38**(4), 2026–2054 (2017). https://doi.org/10.1093/imanum/drx063
24. Meng, J., Mei, L.: A mixed virtual element method for the vibration problem of clamped Kirchhoff plate. Adv. Comput. Math. **46**(5), 68 (2020). https://doi.org/10.1007/s10444-020-09810-1
25. Meng, J., Mei, L.: A C^0 virtual element method for the biharmonic eigenvalue problem. Int. J. Comput. Math. **98**(9), 1821–1833 (2021). https://doi.org/10.1080/00207160.2020.1849635
26. Monzón, G.: A virtual element method for a biharmonic Steklov eigenvalue problem. Adv. Pure Appl. Math. **10**(4), 325–337 (2019). https://doi.org/10.1515/apam-2018-0072
27. Mora, D., Rivera, G., Rodríguez, R.: A virtual element method for the Steklov eigenvalue problem. Math. Models Methods Appl. Sci. **25**(8), 1421–1445 (2015). https://doi.org/10.1007/s10915-021-01555-3
28. Mora, D., Velásquez, I.: A virtual element method for the transmission eigenvalue problem. Math. Models Methods Appl. Sci. **28**(14), 2803–2831 (2018). https://doi.org/10.1142/S0218202518500616
29. Mora, D., Velásquez, I.: Virtual elements for the transmission eigenvalue problem on polytopal meshes. SIAM J. Sci. Comput. **43**(4), 2425–2447 (2021). https://doi.org/10.1137/20M1347887
30. Mora, D., Rivera, G., Velásquez, I.: A virtual element method for the vibration problem of kirchhoff plates. ESAIM: M2AN **52**(4), 1437–1456 (2018). https://doi.org/10.1051/m2an/2017041
31. Carstensen, C., Gräßle, B.: Rate-optimal higher-order adaptive conforming fem for biharmonic eigenvalue problems on polygonal domains. Comput. Methods Appl. Mech. Engrg. **425**, 116931 (2024). https://doi.org/10.1016/j.cma.2024.116931
32. Feng, J., Wang, S., Bi, H., Yang, Y.: An hp-mixed discontinuous Galerkin method for the biharmonic eigenvalue problem. Appl. Math. Comput. **450**(C) (2023). https://doi.org/10.1016/j.amc.2023.127969
33. Gallistl, D.: Morley finite element method for the eigenvalues of the biharmonic operator **35**(4), 1779–1811 (2014). https://doi.org/10.1093/imanum/dru054
34. Li, H., Yang, Y.: Adaptive morley element algorithms for the biharmonic eigenvalue problem. J. Inequal. Appl. **2018**(1), 55 (2018). https://doi.org/10.1186/s13660-018-1643-9
35. Cangiani, A., Georgoulis, E.H., Pryer, T., Sutton, O.J.: A posteriori error estimates for the virtual element method. Numer. Math. **137**, 857–893 (2017). https://doi.org/10.1007/s00211-017-0891-9
36. Dassi, F., Khot, R., Rubiano, A.E., Ruiz-Baier, R.: A posteriori error analysis of a robust virtual element method for stress-assisted diffusion problems (2025). Available at arXiv:2504.00648
37. Mora, D., Rivera, G., Rodriguez, R.: A posteriori error estimates for a virtual element method for the Steklov eigenvalue problem. Comput. Math. Appl. **74**(9), 2172–2190 (2017). https://doi.org/10.1016/j.camwa.2017.05.016
38. Munar, M., Cangiani, A., Velásquez, I.: Residual-based a posteriori error estimation for mixed virtual element methods. Comput. Math. Appl. **166**, 182–197 (2024). https://doi.org/10.1016/j.camwa.2024.05.011
39. Chen, M., Huang, J., Lin, S.: A posteriori error estimation for a C^1 virtual element method of kirchhoff plates **120**, 132–150 (2022). https://doi.org/10.1016/j.camwa.2022.05.001

40. Dassi, F.: VEM++, a C++ library to handle and play with the virtual element method. Numer. Algorithms, 1–43 (2025). https://doi.org/10.1007/s11075-025-02059-z
41. Adams, R.A., Fournier, J.J.F.: Sobolev Spaces, 2nd edn. Elsevier/Academic Press, Amsterdam, Netherlands (2003)
42. Mora, D., Rivera, G.: A priori and a posteriori error estimates for a virtual element spectral analysis for the elasticity equations. IMA J. Numer. Anal. (2019). https://doi.org/10.1093/imanum/dry063
43. Grisvard, P.: Elliptic Problems in Nonsmooth Domains. SIAM, Philadelphia, PA (2011). https://doi.org/10.1137/1.9781611972030
44. Mora, D., Rivera, G., Rodríguez, R.: A posteriori error estimates for a virtual element method for the Steklov eigenvalue problem. Comput. Math. Appl. **74**(9), 2172–2190 (2017). https://doi.org/10.1016/j.camwa.2017.05.016
45. Verfürth, R.: A Review of A Posteriori Error Estimation and Adaptive Mesh-Refinement Techniques. Advances in Numerical Mathematics. Wiley-Teubner, Stuttgart (1996)
46. Zhao, J., Mao, S., Zhang, B., Wang, F.: The interior penalty virtual element method for the biharmonic problem. Math. Comput. **92**(342), 1543–1574 (2023). https://doi.org/10.1090/mcom/3828
47. Dong, Z., Mascotto, L., Sutton, O.J.: Residual-based a posteriori error estimates for hp-discontinuous Galerkin discretizations of the biharmonic problem. SIAM J. Numer. Anal. **59**(3), 1273–1298 (2021). https://doi.org/10.1137/20M1364114
48. Verfürth, R.: A Posteriori Error Estimation Techniques for Finite Element Methods. Oxford University Press, Oxford (2013). https://doi.org/10.1093/acprof:oso/9780199679423.001.0001
49. Hernández, V., Román, J.E., Vidal, V.: SLEPc: Scalable library for eigenvalue problem computations. In: Palma, J.M.L.M., Sousa, A.A., Dongarra, J., Hernández, V. (eds.), High Performance Computing for Computational Science — VECPAR 2002, pp. 377–391. Springer, Berlin, Heidelberg (2003). https://doi.org/10.1007/3-540-36569-9_25
50. Yu, Y.: Implementation of polygonal mesh refinement in MATLAB (2021). Available at arXiv:2101.03456
51. Burstedde, C., Wilcox, L.C., Ghattas, O.: `p4est`: scalable algorithms for parallel adaptive mesh refinement on forests of octrees. SIAM J. Sci. Comput. **33**(3), 1103–1133 (2011). https://doi.org/10.1137/100791634
52. Badia, S., Verdugo, F.: Gridap: an extensible finite element toolbox in Julia. J. Open Source Softw. **5**(52), 2520 (2020). https://doi.org/10.21105/joss.02520
53. Bjørstad, P.E., Tjøstheim, B.P.: High precision solutions of two fourth order eigenvalue problems. Computing **63**(2), 97–107 (1999). https://doi.org/10.1007/s006070050053
54. Feng, J., Wang, S., Bi, H., Yang, Y.: The a posteriori error estimates of the Ciarlet-Raviart mixed finite element method for the biharmonic eigenvalue problem. AIMS Mathematics **9**(2), 3332–3348 (2024). https://doi.org/10.3934/math.2024163
55. Hu, J., Yang, X.: Lower bounds of eigenvalues of the biharmonic operators by the rectangular Morley element methods. Numer. Methods Partial Differential Equations **31**(5), 1623–1644 (2015). https://doi.org/10.1002/num.21964

Publisher's Note Springer Nature remains neutral with regard to jurisdictional claims in published maps and institutional affiliations.